# A MULTISCALE MORTAR MIXED FINITE ELEMENT METHOD*

TODD ARBOGAST†, GERGINA PENCHEVA‡, MARY F. WHEELER§, AND IVAN YOTOV¶

**Abstract.** We develop multiscale mortar mixed finite element discretizations for second order elliptic equations. The continuity of flux is imposed via a mortar finite element space on a course grid scale, while the equations in the coarse elements (or subdomains) are discretized on a fine grid scale. The polynomial degree of the mortar and subdomain approximation spaces may differ; in fact, the mortar space achieves approximation comparable to the fine scale on its coarse grid by using higher order polynomials. Our formulation is related to, but more flexible than, existing multiscale finite element and variational multiscale methods. We derive *a priori* error estimates and show, with appropriate choice of the mortar space, optimal order convergence and some superconvergence on the fine scale for both the solution and its flux. We also derive efficient and reliable *a posteriori* error estimators, which are used in an adaptive mesh refinement algorithm to obtain appropriate subdomain and mortar grids. Numerical experiments are presented in confirmation of the theory.

**Key words.** Multiscale, mixed finite element, mortar finite element, error estimates, *a posteriori,* superconvergence, multiblock, non-matching grids

**AMS subject classifications.** 65N06, 65N12, 65N15, 65N22, 65N30

**1. Introduction.** We consider a second order linear elliptic equation that, in porous medium applications, models single phase Darcy flow. We solve for the pressure $p$ and the velocity $\mathbf{u}$ satisfying

$$\mathbf{u} = -K\nabla p \quad \text{in } \Omega, \tag{1.1}$$

$$\nabla \cdot \mathbf{u} = f \quad \text{in } \Omega, \tag{1.2}$$

$$p = g \quad \text{on } \partial\Omega, \tag{1.3}$$

where $\Omega \subset \mathbf{R}^d$, $d = 2$ or 3, is the domain and $K$ is a symmetric, uniformly positive definite tensor with $L^\infty(\Omega)$ components representing the permeability divided by the viscosity. The Dirichlet boundary conditions are considered merely for simplicity. We suppose that the problem is at least $H^{3/2+\varepsilon}$-regular, for some $\varepsilon > 0$, where $H^r$ is the standard Sobolev space of functions having $r$th order weak derivatives in $L^2$. We have $H^2$-regularity, for example, if $f \in L^2(\Omega)$, $g \in H^{3/2}(\Omega)$, the components of $K \in C^{0,1}(\bar{\Omega})$, and $\Omega$ is convex or $\partial\Omega$ is smooth enough (see [28, 34, 26]).

A number of papers deal with the analysis and implementation of mixed methods applied to the problem on conforming grids (see, e.g., [42, 39, 37, 15, 13, 14, 17, 21, 36, 43, 22, 24, 8, 6] and the books [40, 16]), on nested locally refined grids (see, e.g., [23, 25]), and on nonmatching grids [5, 9]. Another set of papers deals with multiscale

*The first author was supported by National Science Foundation grant DMS–0408489, the third author was supported by the Department of Energy grant DE-FGO2-04ER25617, and the second and forth authors were supported by the NSF grant DMS 0411694 and the DOE grant DE-FG02-04ER25618.

†Institute for Computational Engineering & Sciences and Department of Mathematics, The University of Texas at Austin, Austin, TX 78712; arbogast@ices.utexas.edu.

‡Department of Mathematics, 301 Thackeray Hall, University of Pittsburgh, Pittsburgh, PA 15260; gepst12@math.pitt.edu.

§Institute for Computational Engineering & Sciences, Department of Aerospace Engineering & Engineering Mechanics, and Department of Petroleum & Geosystems Engineering, The University of Texas at Austin, Austin, TX 78712; mfw@ices.utexas.edu.

¶Department of Mathematics, 301 Thackeray Hall, University of Pittsburgh, Pittsburgh, PA 15260; yotov@math.pitt.edu.

approximation of the mixed system (see, e.g., [7, 18, 3, 1, 4, 2] and the related control volume work [33]).

It is difficult to solve (1.1)–(1.3) when $\Omega$ is large and the coefficient $K$ is heterogeneous, varying on a fine scale. A straightforward approach to discretization would require full fine scale grid resolution of the variation in $K$ over all of $\Omega$, resulting in a large, highly coupled system of equations. Solution of this system would in many cases be computationally intractable.

To alleviate the computational burden, the variational multiscale method [31, 32, 12] and multiscale finite elements [29, 30] were developed for (1.1)–(1.3) written as a single second order partial differential equation. The mixed system of two first order equations was treated in a variational multiscale context in [7, 3, 1, 4, 2], and in a multiscale finite element method context in [18]. Up to relatively minor differences, these two approaches are equivalent [4].

In both methods, the problem (1.1)–(1.3) is decomposed into a series of small, local, coarse element (or subdomain) problems. These local problems are given appropriate boundary conditions and solved on the fine scale (to resolve variations in $K$) to define the coarse scale multiscale finite element basis. This coarse basis is then used to approximate the solution globally. Essentially, the problem is fully resolved on the fine scale, but the overall problem is solved using a reduced degree-of-freedom globally coupled system. The computational efficiency of the method comes from its divide-and-conquer strategy. The small, localized subproblems are much more effectively solved than the full system all at once. The coarse scale coupling involving only a few degrees-of-freedom per coarse element edge (or face) also results in a relatively small and easily solved system.

In this paper we develop a new but similar multiscale approach based on domain decomposition theory [27] and mortar finite elements [11, 5]. The idea is simple: we divide $\Omega$ into a series of small subdomains (or coarse elements), over which we pose the original problem. We tie these together using a low degree-of-freedom mortar space defined on a coarse scale mortar grid. The mortar provides a natural Dirichlet pressure boundary condition for the subdomain problems, which can be solved easily because of their relatively small size. The (weak) velocity flux mismatch provides a criterion for updating the mortar pressure, adn we iterate to convergence. By using a higher order mortar approximation, we are able to compensate for the coarseness of the grid scale and maintain good (fine scale) overall accuracy. This approach is more flexible than the variational multiscale method and multiscale finite elements, because it is easy to improve global accuracy by simply refining the local mortar grid where needed. That is, we can easily exploit adaptive meshing strategies to improve where necessary the strength of the global coupling.

Our method is formulated in the next section. After defining some projection operators in §3, we prove *a priori* error bounds in §4. If $h$ resolves the fine scale, and $H > h$ is the coarse mortar scale, and if $m$ is the degree of the mortar approximating polynomials and $k = l$ is the order of the approximation for velocities and pressures, then we show that the velocity errors are $\mathcal{O}(H^{m+1/2} + h^{k+1})$ and the pressure errors are $\mathcal{O}(H^{m+3/2} + h^{k+1})$. Thus, if $m > k$, we can control the mortar error and prevent pollution of the solution. We also show several superconvergence estimates and estimates of the mortar pressure approximation itself.

In §5, we turn our attention to *a posteriori* error estimation, so that we can control an adaptive mesh procedure for obtaining appropriate coarse mortar and fine subdomain grids. Finally, in §6, we present the results of several numerical experiments that confirm and illustrate our theoretical results.

**2. Formulation of the method.** Let $\Omega$ be decomposed into non overlapping subdomain blocks $\Omega_i$, so that $\overline{\Omega} = \cup_{i=1}^n \overline{\Omega}_i$ and $\Omega_i \cap \Omega_j = \emptyset$ for $i \neq j$. Let $\Gamma_{i,j} = \partial\Omega_i \cap \partial\Omega_j$, $\Gamma = \cup_{1\le i<j\le n}\Gamma_{i,j}$, and $\Gamma_i = \partial\Omega_i \cap \Gamma = \partial\Omega_i \backslash \partial\Omega$ denote interior block interfaces. Let

$$\begin{aligned}
\mathbf{V}_i &= H(\mathrm{div};\Omega_i), & \mathbf{V} &= \bigoplus_{i=1}^n \mathbf{V}_i,\\
W_i &= L^2(\Omega_i), & W &= \bigoplus_{i=1}^n W_i = L^2(\Omega),\\
M_{i,j} &= H^{1/2}(\Gamma_{i,j}), & M &= \bigoplus_{1\le i<j\le n} M_{i,j}.
\end{aligned}$$

Following [5], a weak form of (1.1)–(1.3) asks for $\mathbf{u} \in \mathbf{V}$, $p \in W$, and $\lambda \in M$ such that, for each $i$,

$$(K^{-1}\mathbf{u},\mathbf{v})_{\Omega_i} = (p,\nabla\cdot\mathbf{v})_{\Omega_i} - \langle \lambda, \mathbf{v}\cdot\nu_i\rangle_{\Gamma_i} - \langle g, \mathbf{v}\cdot\nu_i\rangle_{\partial\Omega_i\backslash\Gamma}, \quad \mathbf{v}\in\mathbf{V}_i, \tag{2.1}$$

$$(\nabla\cdot\mathbf{u}, w)_{\Omega_i} = (f,w)_{\Omega_i}, \quad w \in W_i, \tag{2.2}$$

$$\sum_{i=1}^n \langle \mathbf{u}\cdot\nu_i, \mu\rangle_{\Gamma_i} = 0, \quad \mu \in M, \tag{2.3}$$

where $\nu_i$ is the outer unit normal to $\partial\Omega_i$ (see also [16, pp. 91–92]). Note that $\lambda$ is the pressure on the block interfaces $\Gamma$, and that (2.3) enforces weak continuity of $\mathbf{u}\cdot\nu$ on each $\Gamma_{i,j}$.

**2.1. The finite element approximation.** Let $\mathcal{T}_{h,i}$ be a conforming, quasi-uniform affine finite element partition of $\Omega_i$, $1 \le i \le n$, of maximal element diameter $h_i$. Let $h = \max_{1\le i\le n} h_i$. Note that we allow for the possibility that $\mathcal{T}_{h,i}$ and $\mathcal{T}_{h,j}$ need not align on $\Gamma_{i,j}$. Define $\mathcal{T}_h = \cup_{i=1}^n \mathcal{T}_{h,i}$ and let $\mathcal{E}_h$ be the union of all interior edges (or faces in three dimensions) not including the subdomain interfaces and the outer boundary. Let

$$\mathbf{V}_{h,i} \times W_{h,i} \subset \mathbf{V}_i \times W_i$$

be any of the usual mixed finite element spaces (e.g., those of [42, 39, 37, 15, 14, 13, 17]), and let $\mathbf{V}_h$ or, equivalently, $\mathbf{V}_h\cdot\nu$ contain the polynomials of degree $k$. Then let

$$\mathbf{V}_h = \bigoplus_{i=1}^n \mathbf{V}_{h,i}, \qquad W_h = \bigoplus_{i=1}^n W_{h,i}.$$

Note that the normal components of vectors in $\mathbf{V}_h$ are continuous between elements within each block $\Omega_i$, but not across $\Gamma$.

Let the mortar interface mesh $\mathcal{T}_{H,i,j}$ be a quasi-uniform finite element partition of $\Gamma_{i,j}$ with maximal element diameter $H_{i,j}$. Let $H = \max_{1\le i,j\le n} H_{i,j}$. Define $\mathcal{T}^{\Gamma,H} = \cup_{1\le i<j\le n}\mathcal{T}_{H,i,j}$. For any $\tau \in \mathcal{T}_{H,i,j}$, let

$$E_\tau = \big\{E \in \mathcal{T}_h : \partial E \cap \tau \neq \emptyset\big\}.$$

Denote by $M_{H,i,j} \subset L^2(\Gamma_{i,j})$ the mortar space on $\Gamma_{i,j}$, containing either the continuous or discontinuous piecewise polynomials of degree $m$ on $\mathcal{T}_{H,i,j}$, where $m$ is at least $k+1$.

We remark that $\mathcal{T}_{H,i,j}$ need not be conforming if $M_{H,i,j}$ is discontinuous, but our error analysis will require conformity. Now let

$$M_H = \bigoplus_{1\le i<j\le n} M_{H,i,j}$$

be the mortar finite element space on $\Gamma$. For each subdomain $\Omega_i$, define a projection $\mathcal{Q}_{h,i} : L^2(\Gamma_i) \to \mathbf{V}_{h,i} \cdot \nu_i|_{\Gamma_i}$ such that, for any $\phi \in L^2(\Gamma_i)$,

$$\langle \phi - \mathcal{Q}_{h,i}\phi, \mathbf{v}\cdot\nu_i\rangle_{\Gamma_i} = 0, \quad \mathbf{v} \in \mathbf{V}_{h,i}. \tag{2.4}$$

We require that the following condition be satisfied [5], where in this paper $\|\cdot\|_{r,R}$ is the usual Sobolev norm of $H^r(R)$ (we may drop $r$ if $r = 0$ and $R$ if $R = \Omega$).

ASSUMPTION 2.1. *Assume that there exists a constant $C$, independent of $h$ and $H$, such that*

$$\|\mu\|_{\Gamma_{i,j}} \le C(\|\mathcal{Q}_{h,i}\mu\|_{\Gamma_{i,j}} + \|\mathcal{Q}_{h,j}\mu\|_{\Gamma_{i,j}}), \quad \mu \in M_H,\ \ 1 \le i < j \le n. \tag{2.5}$$

Condition (2.5) says that the mortar space cannot be too rich compared to the normal traces of the subdomain velocity spaces. Therefore in the sequel, we tacitly assume that $h \le H \le 1$. Condition (2.5) is not a very restrictive, and it is easily satisfied in practice (see, e.g., [46, 38]). In the following we treat any function $\mu \in M_H$ as extended by zero on $\partial\Omega$.

In the mixed finite element approximation of (2.1)–(2.2), we seek $\mathbf{u}_h \in \mathbf{V}_h$, $p_h \in W_h$, $\lambda_H \in M_H$ such that, for $1 \le i \le n$,

$$(K^{-1}\mathbf{u}_h, \mathbf{v})_{\Omega_i} = (p_h, \nabla\cdot\mathbf{v})_{\Omega_i} - \langle\lambda_H, \mathbf{v}\cdot\nu_i\rangle_{\Gamma_i} - \langle g, \mathbf{v}\cdot\nu_i\rangle_{\partial\Omega_i\setminus\Gamma}, \quad \mathbf{v} \in \mathbf{V}_{h,i}, \tag{2.6}$$

$$(\nabla\cdot\mathbf{u}_h, w)_{\Omega_i} = (f, w)_{\Omega_i}, \qquad w \in W_{h,i}, \tag{2.7}$$

$$\sum_{i=1}^n \langle \mathbf{u}_h\cdot\nu_i, \mu\rangle_{\Gamma_i} = 0, \qquad \mu \in M_H. \tag{2.8}$$

Strictly within each block $\Omega_i$, we have a standard mixed finite element method, and (2.7) enforces local conservation over each grid cell. Moreover, $\mathbf{u}_h\cdot\nu$ is continuous on any element edge (or face) $e \not\subset \Gamma\cup\partial\Omega$, and (2.8) enforces weak continuity of flux across these interfaces with respect to the mortar space $M_H$.

The above method was defined in [5], except that $H$ was comparable to $h$ ($H = \mathcal{O}(h)$) and $m = k+1$ was one more than the degree of approximating polynomials in $\mathbf{V}_h$. In the present work, we weaken the discretization of $\Gamma$ by taking larger elements of size $H$ but compensating with a higher degree of approximation. The theoretical results of [5] no longer hold, since asymptotically we now take $H = \mathcal{O}(h^\alpha)$, with $\alpha < 1$.

**2.2. A domain decomposition formulation.** Define a bilinear form $d_H : L^2(\Gamma)\times L^2(\Gamma) \to \mathbf{R}$ by

$$d_H(\lambda,\mu) = \sum_{i=1}^n d_{H,i}(\lambda,\mu) = -\sum_{i=1}^n \langle \mathbf{u}_h^*(\lambda)\cdot\nu_i, \mu\rangle_{\Gamma_i},$$

where $(\mathbf{u}_h^*(\lambda), p_h^*(\lambda)) \in \mathbf{V}_h \times W_h$ solves

$$(K^{-1}\mathbf{u}_h^*(\lambda), \mathbf{v})_{\Omega_i} = (p_h^*(\lambda), \nabla\cdot\mathbf{v})_{\Omega_i} - \langle\lambda, \mathbf{v}\cdot\nu_i\rangle_{\Gamma_i}, \quad \mathbf{v} \in \mathbf{V}_{h,i}, \tag{2.9}$$

$$(\nabla\cdot\mathbf{u}_h^*(\lambda), w)_{\Omega_i} = 0, \qquad w \in W_{h,i}, \tag{2.10}$$

for each $1 \le i \le n$. Also define a linear functional $g_H : L^2(\Gamma) \to \mathbf{R}$ by

$$g_H(\mu) = \sum_{i=1}^{n} g_{H,i}(\mu) = \sum_{i=1}^{n} \langle \bar{\mathbf{u}}_h \cdot \nu_i, \mu \rangle_{\Gamma_i},$$

where $(\bar{\mathbf{u}}_h, \bar{p}_h) \in \mathbf{V}_h \times W_h$ solves, for $1 \le i \le n$,

$$(K^{-1}\bar{\mathbf{u}}_h, \mathbf{v})_{\Omega_i} = (\bar{p}_h, \nabla \cdot \mathbf{v})_{\Omega_i} - \langle g, \mathbf{v} \cdot \nu_i \rangle_{\partial\Omega_i \setminus \Gamma}, \quad \mathbf{v} \in \mathbf{V}_{h,i}, \tag{2.11}$$

$$(\nabla \cdot \bar{\mathbf{u}}_h, w)_{\Omega_i} = (f, w)_{\Omega_i}, \quad w \in W_{h,i}. \tag{2.12}$$

It is straightforward to show (see [27, 5]) that the solution of

$$d_H(\lambda_H, \mu) = g_H(\mu), \quad \mu \in M_H, \tag{2.13}$$

generates the solution of (2.6)–(2.8) via

$$\mathbf{u}_h = \mathbf{u}_h^*(\lambda_H) + \bar{\mathbf{u}}_h, \qquad p_h = p_h^*(\lambda_H) + \bar{p}_h. \tag{2.14}$$

The following is proved in [5].

Lemma 2.1. *The interface bilinear form $d_H(\cdot,\cdot)$ is symmetric and positive semi-definite on $L^2(\Gamma)$. If (2.5) holds, then $d_H(\cdot,\cdot)$ is positive definite on $M_H$. Moreover,*

$$d_{H,i}(\mu, \mu) = (K^{-1}\mathbf{u}_h^*(\mu), \mathbf{u}_h^*(\mu))_{\Omega_i} \ge 0. \tag{2.15}$$

A substructuring domain decomposition algorithm based on an algorithm of Glowinski and Wheeler [27] can be used to solve the linear system of equations resulting from (2.6)–(2.8) very efficiently in parallel. See [5] for more details.

**3. Some projection operators and the weakly continuous velocities.** We first introduce some projection operators needed in the analysis. Let $\mathcal{I}_H^c$ be the nodal interpolant operator into the space $M_H^c$, which is the subset of continuous functions in $M_H$ (where we must use the Scott-Zhang [41] operator to define the nodal values of $\psi$ if $\psi$ is not smooth enough to form $\mathcal{I}_H^c\psi$ directly). For any $\varphi \in L^2(\Omega)$, let $\hat{\varphi} \in W_h$ be its $L^2(\Omega)$-projection satisfying

$$(\varphi - \hat{\varphi}, w) = 0, \quad w \in W_h.$$

Similarly, let $\mathcal{P}_H$ denote the $L^2(\Gamma)$ projection into $M_H$. We have already (2.4), which defines the projection $\mathcal{Q}_{h,i} : L^2(\Gamma_i) \to \mathbf{V}_{h,i} \cdot \nu_i|_{\Gamma_i}$.

We recall that, for any of the standard mixed spaces,

$$\nabla \cdot \mathbf{V}_{h,i} = W_{h,i},$$

and there exists a projection $\Pi_i$ of $(H^\varepsilon(\Omega_i))^d \cap \mathbf{V}_i$ onto $\mathbf{V}_{h,i}$ (for any $\varepsilon > 0$), satisfying that for any $\mathbf{q} \in (H^\varepsilon(\Omega_i))^d \cap \mathbf{V}_i$,

$$\nabla \cdot \Pi_i \mathbf{q} = \widehat{\nabla \cdot \mathbf{q}}, \tag{3.1}$$

$$(\Pi_i \mathbf{q}) \cdot \nu_i = \mathcal{Q}_{h,i}(\mathbf{q} \cdot \nu_i). \tag{3.2}$$

Moreover (see [35, 5]),

$$\|\Pi_i \mathbf{q}\|_{\Omega_i} \le C(\|\mathbf{q}\|_{\varepsilon,\Omega_i} + \|\nabla \cdot \mathbf{q}\|_{\Omega_i}). \tag{3.3}$$

We assume that the order of approximation of $W_{h,i}$ is $l+1$ (and recall that $\mathbf{V}_{h,i}$ is $k+1$ and $M_H$ is $m+1$). In all cases, $l = k$ or $l = k-1$, and we have assumed for simplicity that the order of approximation is the same on every subdomain. Our projection operators have the following approximation properties:

$$\|\psi - \mathcal{I}_H^c \psi\|_{t,\Gamma_{i,j}} \le C\|\psi\|_{s,\Gamma_{i,j}} H^{s-t}, \qquad 0 \le s \le m+1,\ 0 \le t \le 1, \tag{3.4}$$

$$\|\psi - \mathcal{P}_H \psi\|_{-t,\Gamma_{i,j}} \le C\|\psi\|_{s,\Gamma_{i,j}} H^{s+t}, \qquad 0 \le s \le m+1,\ 0 \le t \le 1, \tag{3.5}$$

$$\|\varphi - \hat{\varphi}\| \le C\|\varphi\|_t h^t, \qquad 0 \le t \le l+1, \tag{3.6}$$

$$\|\nabla\cdot(\mathbf{q} - \Pi_i \mathbf{q})\|_{\Omega_i} \le C\|\nabla\cdot\mathbf{q}\|_{t,\Omega_i} h^t, \qquad 0 \le t \le l+1, \tag{3.7}$$

$$\|\mathbf{q} - \Pi_i \mathbf{q}\|_{\Omega_i} \le C\|\mathbf{q}\|_{r,\Omega_i} h^r, \qquad 1 \le r \le k+1, \tag{3.8}$$

$$\|\psi - \mathcal{Q}_{h,i}\psi\|_{-t,\Gamma_{i,j}} \le C\|\psi\|_{r,\Gamma_{i,j}} h^{r+t}, \qquad 0 \le r \le k+1,\ 0 \le t \le k+1, \tag{3.9}$$

$$\|(\mathbf{q} - \Pi_i \mathbf{q})\cdot\nu_i\|_{-t,\Gamma_{i,j}} \le C\|\mathbf{q}\|_{r,\Gamma_{i,j}} h^{r+t}, \qquad 0 \le r \le k+1,\ 0 \le t \le k+1, \tag{3.10}$$

where $\|\cdot\|_{-t}$ is the norm of $H^{-t}$, the dual of $H^t$ (*not* $H_0^t$). Bounds (3.5)–(3.7) and (3.9)–(3.10) are standard $L^2$-projection approximation results [19]; bound (3.8) can be found in [16, 40]; and (3.4) is a standard interpolation bound [19].

For theoretical purposes it is convenient to define the space of weakly continuous velocities, which is the space

$$\mathbf{V}_{h,0} = \left\{ \mathbf{v} \in \mathbf{V}_h : \sum_{i=1}^n \langle \mathbf{v}|_{\Omega_i}\cdot\nu_i, \mu\rangle_{\Gamma_i} = 0 \ \ \forall\ \ \mu \in M_H \right\}.$$

We note that we can eliminate $\lambda_H$ from the mixed method (2.6)–(2.8) by restricting $\mathbf{V}_h$ to $\mathbf{V}_{h,0}$; that is, the problem is equivalent to finding $\mathbf{u}_h \in \mathbf{V}_{h,0}$ and $p_h \in W_h$ such that

$$(K^{-1}\mathbf{u}_h, \mathbf{v}) = \sum_{i=1}^n (p_h, \nabla\cdot\mathbf{v})_{\Omega_i} - \langle g, \mathbf{v}\cdot\nu\rangle_{\partial\Omega}, \quad \mathbf{v} \in \mathbf{V}_{h,0}, \tag{3.11}$$

$$\sum_{i=1}^n (\nabla\cdot\mathbf{u}_h, w)_{\Omega_i} = (f, w), \qquad w \in W_h. \tag{3.12}$$

LEMMA 3.1. *Under hypothesis* (2.5), *there exists a projection operator* $\Pi_0 : (H^{1/2+\varepsilon}(\Omega)) \cap \mathbf{V} \to \mathbf{V}_{h,0}$ *such that*

$$(\nabla\cdot(\Pi_0\mathbf{q} - \mathbf{q}), w)_\Omega = 0, \quad w \in W_h, \tag{3.13}$$

*and*

$$\|\Pi_0\mathbf{q} - \Pi\mathbf{q}\| \le C\sum_{i=1}^n \|\mathbf{q}\|_{r+1/2,\Omega_i} h^r H^{1/2}, \qquad 0 \le r \le k+1, \tag{3.14}$$

$$\|\Pi_0\mathbf{q} - \mathbf{q}\| \le C\sum_{i=1}^n \big(\|\mathbf{q}\|_{r,\Omega_i} h^r + \|\mathbf{q}\|_{r+1/2,\Omega_i} h^r H^{1/2}\big), \quad 1 \le r \le k+1, \tag{3.15}$$

$$\|\Pi_0\mathbf{q} - \mathbf{q}\| \le C\sum_{i=1}^n \|\mathbf{q}\|_{r,\Omega_i} h^{r-1/2} H^{1/2}, \qquad 1 \le r \le k+1, \tag{3.16}$$

*wherein* $\Pi\mathbf{q}|_{\Omega_i} = \Pi_i\mathbf{q}$.

The proof of this lemma can be found in [5, §3], with a straightforward modification of the argument for the two scales $h$ and $H$. It is now easy to prove solvability of our method.

LEMMA 3.2. *If* (2.5) *holds, then there exists a unique solution of* (2.6)–(2.8).

*Proof.* Uniqueness for vanishing data implies general existence and uniqueness for finite dimensional square linear systems, so assume $f$ and $g$ vanish. Take $\mathbf{v} = \mathbf{u}_h \in \mathbf{V}_{h,0}$ in (3.11)–(3.12) to conclude that $\mathbf{u}_h = 0$. Given $p_h \in W_h$, there is a vector field $\mathbf{q}$ such that $\nabla \cdot \mathbf{q} = p_h$, so take $\mathbf{v} = \Pi_0 \mathbf{q}$ to conclude that $0 = \sum_i (p_h, \nabla \cdot \Pi_0 \mathbf{q})_{\Omega_i} = (p_h, \nabla \cdot \mathbf{q})_\Omega = \|p_h\|^2$, implying that $p_h = 0$. Now returning to (2.6), we have that $0 = \langle \lambda_H, \mathbf{v} \cdot \nu_i \rangle_{\Gamma_i} = \langle \mathcal{Q}_{h,i}\lambda_H, \mathbf{v} \cdot \nu_i \rangle_{\Gamma_i}$ for any $\mathbf{v} \in \mathbf{V}_{h,i}$. Again, we can find some $\mathbf{v}$ so that $\mathbf{v} \cdot \nu_i = \mathcal{Q}_{h,i}\lambda_H$, which implies that $\mathcal{Q}_{h,i}\lambda_H = 0$. Finally, (2.5) shows that $\lambda_H = 0$ and the proof is complete. ∎

In the analysis, we will use the nonstandard trace theorem

$$\|q\|_{r,\Gamma_{i,j}} \le C \|q\|_{r+1/2,\Omega_i} \tag{3.17}$$

(see [28, Theorem 1.5.2.1]), the local inverse inequality

$$\|\mathbf{v} \cdot \nu\|_{\partial\Omega_i} \le C h^{-1/2} \|\mathbf{v}\|_{\Omega_i} \tag{3.18}$$

for any function $\mathbf{v} \in \mathbf{V}_{h,i}$ (see [5, Lemma 4.1]), and the bound (see [39, 16])

$$\langle q, \mathbf{v} \cdot \nu \rangle_{\partial\Omega_i} \le C \|q\|_{1/2,\partial\Omega_i} \|\mathbf{v}\|_{H(\mathrm{div};\Omega_i)}. \tag{3.19}$$

**4. *A priori* error estimates.** Subtracting (3.11)–(3.12) from (2.1)–(2.2) gives the following equations for the error (recall that $\lambda = p$):

$$(K^{-1}(\mathbf{u} - \mathbf{u}_h), \mathbf{v}) = \sum_{i=1}^{n} \big( (p - p_h, \nabla \cdot \mathbf{v})_{\Omega_i} - \langle p, \mathbf{v} \cdot \nu_i \rangle_{\Gamma_i} \big), \quad \mathbf{v} \in \mathbf{V}_{h,0}, \tag{4.1}$$

$$\sum_{i=1}^{n} (\nabla \cdot (\mathbf{u} - \mathbf{u}_h), w)_{\Omega_i} = 0, \qquad w \in W_h. \tag{4.2}$$

**4.1. *A priori* estimates for the velocity.**

THEOREM 4.1. *For the velocity* $\mathbf{u}_h$ *of the mixed method* (2.6)–(2.8), *if* (2.5) *holds, then there exists a positive constant* $C$, *independent of* $h$ *and* $H$, *such that*

$$\|\nabla \cdot (\mathbf{u} - \mathbf{u}_h)\| \le C \sum_{i=1}^{n} \|\nabla \cdot \mathbf{u}\|_{r,\Omega_i} h^r, \quad 0 \le r \le l+1, \tag{4.3}$$

$$\begin{aligned} \|\mathbf{u} - \mathbf{u}_h\| \le C \sum_{i=1}^{n} \big( &\|p\|_{s+1/2,\Omega_i} H^{s-1/2} + \|\mathbf{u}\|_{r,\Omega_i} h^r \\ &+ \|\mathbf{u}\|_{r+1/2,\Omega_i} h^r H^{1/2} \big), \quad 1 \le r \le k+1,\ 0 \le s \le m+1. \end{aligned} \tag{4.4}$$

REMARK 4.1. A straightforward modification of the argument in [5, §4] produces error estimates for $\|\mathbf{u} - \mathbf{u}_h\|$ of order $\mathcal{O}(H^s h^{-1/2} + h^r)$, which at its limits is $\mathcal{O}(H^{m+1} h^{-1/2} + h^{k+1})$. This is asymptotically undesirable as $h \to 0$. In our improved estimate, we obtain a balancing of the terms in (4.4) when $H = \mathcal{O}(h^{r/(s-1/2)})$, which at its limits is $H = \mathcal{O}(h^{(k+1)/(m+1/2)})$. For the lowest order Raviart-Thomas-Nedelec space $\mathrm{RTN}_0$ [39, 37], $k = l = 0$ and so if, say, $m = 2$, then we should take the asymptotic scaling $H = \mathcal{O}(h^{2/5})$, which maintains the optimal convergence rate $\mathcal{O}(h)$.

*Proof.* The divergence error is trivial to estimate from (4.2) using $w = \nabla \cdot (\Pi\mathbf{u} - \mathbf{u}_h) \in W_h$ and (3.7). Note also that $\nabla \cdot \Pi_0\mathbf{u} = \nabla \cdot \mathbf{u}_h = \hat{f} = \widehat{\nabla \cdot \mathbf{u}}$.

We take $\mathbf{v} = \Pi_0\mathbf{u} - \mathbf{u}_h \in \mathbf{V}_{h,0}$ and $w = \hat{p} - p_h$ in (4.1)–(4.2), sum the equations, and note that $\sum_i \langle \mathcal{I}_H^c p, \mathbf{v} \cdot \nu_i \rangle_{\Gamma_i} = 0$ for any $\mathbf{v} \in \mathbf{V}_{h,0}$ to get

$$
\begin{aligned}
(4.5)\quad & (K^{-1}(\Pi_0\mathbf{u} - \mathbf{u}_h), \Pi_0\mathbf{u} - \mathbf{u}_h) \\
&= \sum_{i=1}^{n} \langle \mathcal{I}_H^c p - p, (\Pi_0\mathbf{u} - \mathbf{u}_h) \cdot \nu_i \rangle_{\Gamma_i} + (K^{-1}(\Pi_0\mathbf{u} - \mathbf{u}), \Pi_0\mathbf{u} - \mathbf{u}_h) \\
&\le \sum_{i=1}^{n} \|\mathcal{I}_H^c p - p\|_{1/2,\partial\Omega_i} \|\Pi_0\mathbf{u} - \mathbf{u}_h\|_{H(\mathrm{div};\Omega_i)} + (K^{-1}(\Pi_0\mathbf{u} - \mathbf{u}), \Pi_0\mathbf{u} - \mathbf{u}_h) \\
&\le C\bigg( \sum_{i=1}^{n} \|p\|_{s+1/2,\Omega_i} H^{s-1/2} \|\Pi_0\mathbf{u} - \mathbf{u}_h\|_{\Omega_i} \\
&\qquad + \sum_{i=1}^{n} \big( \|\mathbf{u}\|_{r,\Omega_i} h^r + \|\mathbf{u}\|_{r+1/2,\Omega_i} h^r H^{1/2} \big) \|\Pi_0\mathbf{u} - \mathbf{u}_h\| \bigg),
\end{aligned}
$$

for $1 \le r \le k+1$, $0 \le s \le m+1$, where we used (3.4), (3.17), and (3.15), and that $\nabla \cdot (\Pi_0\mathbf{u} - \mathbf{u}_h) = 0$. An application of the Cauchy-Schwarz inequality completes the proof. □

If we restrict to the case of diagonal tensor $K$ and Raviart-Thomas-Nedelec (RTN) spaces [39, 37] on rectangular grids, we can obtain superconvergence of the velocity at certain discrete points. For a function $\psi$ and a (say 3-D) rectangular element $E$, let $|||\psi|||_{i,E}^2$ denote the approximate integral of $|\psi|^2$ using exact integration in $x_i$ and the $k+1$ point Gauss rule in the other directions. Then let

$$
(4.6)\qquad |||\mathbf{q}|||^2 = \sum_{i=1}^{3} \sum_{E \in \mathcal{T}_h} |||q_i|||_{i,E}^2,
$$

and note that if $\mathbf{v} \in \mathbf{V}_h$, then $|||\mathbf{v}||| = \|\mathbf{v}\|_\Omega$.

THEOREM 4.2. *Assume that the tensor $K$ is diagonal and the mixed finite element spaces are* RTN *on rectangular grids. For the velocity $\mathbf{u}_h$ of the mixed method* (2.6)–(2.8)*, if* (2.5) *holds, then there exists a positive constant $C$, independent of $h$ and $H$, such that*

$$
(4.7)\qquad |||\mathbf{u} - \mathbf{u}_h||| \le C \sum_{i=1}^{n} \big( \|p\|_{s+1/2,\Omega_i} H^{s-1/2} + \|\mathbf{u}\|_{r+1/2,\Omega_i} h^r H^{1/2} \big),
$$

*where* $1/2 \le r \le k+1$, $0 \le s \le m+1$.

*Proof.* We need two well-known results about superconvergence on the subdomains. First, $\Pi$ is super-close to the weighted $L^2$-projection (see [36] and [22, Theorem 3.1]), which translates into

$$
(K^{-1}(\Pi\mathbf{u} - \mathbf{u}), \Pi_0\mathbf{u} - \mathbf{u}_h)_{\Omega_i} \le C\|\mathbf{u}\|_{r+1,\Omega_i} h^{r+1} \|\Pi_0\mathbf{u} - \mathbf{u}_h\|_{\Omega_i}, \quad 0 \le r \le k+1.
$$

Second, the usual mixed method $\Pi$ operator exhibits superconvergence (see [22]):

$$
(4.8)\qquad |||\mathbf{u} - \Pi\mathbf{u}|||_{\Omega_i} \le C\|\mathbf{u}\|_{r+1,\Omega_i} h^{r+1}, \quad 0 \le r \le k+1.
$$

To use the former estimate, we revisit part of (4.5) and estimate the term

$$
\begin{aligned}
&(K^{-1}(\Pi_0\mathbf{u}-\mathbf{u}),\Pi_0\mathbf{u}-\mathbf{u}_h)_{\Omega_i}\\
&\quad=(K^{-1}(\Pi_0\mathbf{u}-\Pi\mathbf{u}),\Pi_0\mathbf{u}-\mathbf{u}_h)_{\Omega_i}+(K^{-1}(\Pi\mathbf{u}-\mathbf{u}),\Pi_0\mathbf{u}-\mathbf{u}_h)_{\Omega_i}\\
&\quad\le C\big(\|\Pi_0\mathbf{u}-\Pi\mathbf{u}\|_{\Omega_i}+\|\mathbf{u}\|_{r+1/2,\Omega_i}h^{r+1/2}\big)\|\Pi_0\mathbf{u}-\mathbf{u}_h\|_{\Omega_i},
\end{aligned}
$$

for $1/2\le r\le k+3/2$. Thus with (3.14), the bound in (4.5) is improved to

$$
\|\Pi_0\mathbf{u}-\mathbf{u}_h\|\le C\sum_{i=1}^{n}\big(\|p\|_{s+1/2,\Omega_i}H^{s-1/2}+\|\mathbf{u}\|_{r+1/2,\Omega_i}h^rH^{1/2}\big), \tag{4.9}
$$

where $1/2\le r\le k+1$ and $0\le s\le m+1$. Finally,

$$
\begin{aligned}
|||\mathbf{u}-\mathbf{u}_h|||&\le|||\mathbf{u}-\Pi\mathbf{u}|||+|||\Pi\mathbf{u}-\Pi_0\mathbf{u}|||+|||\Pi_0\mathbf{u}-\mathbf{u}_h|||\\
&=|||\mathbf{u}-\Pi\mathbf{u}|||+\|\Pi\mathbf{u}-\Pi_0\mathbf{u}\|+\|\Pi_0\mathbf{u}-\mathbf{u}_h\|,
\end{aligned}
$$

so a combination of the above estimates and (3.14) completes the proof. ∎

REMARK 4.2. For $\mathrm{RTN}_0$ ($k=l=0$), the terms in (4.7) are balanced if $H=\mathcal{O}(h^{1/m})$, giving the superconvergence error $\mathcal{O}(h^{1+1/2m})$. For $m=2$, this is $H=\mathcal{O}(h^{1/2})$, which differs slightly from the optimal choice $\mathcal{O}(h^{2/5})$ from the Remark 4.1.

### 4.2. *A priori* estimates for the pressure.

THEOREM 4.3. *Assume full $H^2$-regularity of the problem on $\Omega$. For the pressure $p_h$ of the mixed method* (2.6)–(2.8)*, if* (2.5) *holds, then there exists a positive constant $C$, independent of $h$ and $H$, such that*

$$
\begin{aligned}
\|\hat p-p_h\|\le C\sum_{i=1}^{n}\big(&\|p\|_{s+1/2,\Omega_i}H^{s+1/2}+\|\nabla\cdot\mathbf{u}\|_{t,\Omega_i}h^tH\\
&+\|\mathbf{u}\|_{r,\Omega_i}h^rH+\|\mathbf{u}\|_{r+1/2,\Omega_i}h^rH^{3/2}\big),
\end{aligned} \tag{4.10}
$$

$$
\|p-p_h\|\le C\sum_{i=1}^{n}\|p\|_{t,\Omega_i}h^t+\|\hat p-p_h\|, \tag{4.11}
$$

*where $1\le r\le k+1$, $0<s\le m+1$, and $0\le t\le l+1$.*

REMARK 4.3. Again, a straightforward modification of the argument in [5] produces an undesirable superconvergence error estimate of order $\mathcal{O}\big(H^{m+2}h^{-1/2}+H^{3/2}h^{k+1/2}+h^{l+2}\big)$ instead of $\mathcal{O}\big(H^{m+3/2}+H(h^{l+1}+h^{k+1})\big)$. A balancing of the terms in (4.10) implies for spaces with $l=k$ that $H=\mathcal{O}(h^{(k+1)/(m+1/2)})$, which gives superconvergence of order $\mathcal{O}(h^{(k+1)(m+3/2)/(m+1/2)})$. For $k=0$ and $m=2$, we should take the asymptotic scaling $H=\mathcal{O}(h^{2/5})$, which gives $\mathcal{O}(h^{7/5})$. If $H=\mathcal{O}(h^{1/m})$, as in Remark 4.2, then we expect an error of $\mathcal{O}(h^{1+1/m})$ when $k=l=0$.

*Proof.* The proof uses a duality argument. Let $\varphi$ be the solution of

$$
\begin{aligned}
-\nabla\cdot K\nabla\varphi&=-(\hat p-p_h)\quad&&\text{in }\Omega,\\
\varphi&=0&&\text{on }\partial\Omega,
\end{aligned}
$$

and note that by elliptic regularity,

$$
\|\varphi\|_2\le C\|\hat p-p_h\|. \tag{4.12}
$$

Take $\mathbf{v} = \Pi_0 K\nabla\varphi$ in (4.1) and use the weak continuity of $\mathbf{v}$ to see that

$$
\begin{aligned}
\|\hat{p} - p_h\|^2 &= \sum_{i=1}^n (\hat{p} - p_h, \nabla\cdot\Pi_0 K\nabla\varphi)_{\Omega_i} \\
&= \sum_{i=1}^n \big[(K^{-1}(\mathbf{u}-\mathbf{u}_h), \Pi_0 K\nabla\varphi)_{\Omega_i} + \langle p - \mathcal{P}_H p, \Pi_0 K\nabla\varphi\cdot\nu_i\rangle_{\Gamma_i}\big].
\end{aligned}
\tag{4.13}
$$

The first term on the right is easily estimated as

$$
\begin{aligned}
&\sum_{i=1}^n (K^{-1}(\mathbf{u}-\mathbf{u}_h), \Pi_0 K\nabla\varphi)_{\Omega_i} \\
&\quad = \sum_{i=1}^n \big[(K^{-1}(\mathbf{u}-\mathbf{u}_h), \Pi_0 K\nabla\varphi - K\nabla\varphi)_{\Omega_i} + (\mathbf{u}-\mathbf{u}_h, \nabla\varphi)_{\Omega_i}\big] \\
&\quad = \sum_{i=1}^n \big[(K^{-1}(\mathbf{u}-\mathbf{u}_h), \Pi_0 K\nabla\varphi - K\nabla\varphi)_{\Omega_i} \\
&\qquad\quad - (\nabla\cdot(\mathbf{u}-\mathbf{u}_h), \varphi - \hat{\varphi})_{\Omega_i} + \langle(\mathbf{u}-\mathbf{u}_h)\cdot\nu_i, \varphi - \mathcal{P}_H\varphi\rangle_{\Gamma_i}\big] \\
&\quad \le C\sum_{i=1}^n \big(\|\mathbf{u}-\mathbf{u}_h\|_{\Omega_i}\sqrt{hH} + \|\nabla\cdot(\mathbf{u}-\mathbf{u}_h)\|_{\Omega_i} h \\
&\qquad\quad + \|\mathbf{u}-\mathbf{u}_h\|_{H(\mathrm{div};\Omega_i)} H\big)\|\varphi\|_{2,\Omega_i},
\end{aligned}
\tag{4.14}
$$

using (3.16), (3.6), and (3.4), where $C = C(\max_i \|K\|_{1,\infty,\Omega_i})$. For the second term on the right in (4.13) we have

$$
\begin{aligned}
&\langle p - \mathcal{P}_H p, \Pi_0 K\nabla\varphi\cdot\nu_i\rangle_{\Gamma_i} \\
&\quad = \langle p - \mathcal{P}_H p, (\Pi_0 K\nabla\varphi - \Pi_i K\nabla\varphi)\cdot\nu_i + (\Pi_i K\nabla\varphi - K\nabla\varphi)\cdot\nu_i + K\nabla\varphi\cdot\nu_i\rangle_{\Gamma_i} \\
&\quad \le \sum_j \|p - \mathcal{P}_H p\|_{\Gamma_{i,j}}\big(\|(\Pi_0 K\nabla\varphi - \Pi_i K\nabla\varphi)\cdot\nu_i\|_{\Gamma_{i,j}} \\
&\qquad + \|(\Pi_i K\nabla\varphi - K\nabla\varphi)\cdot\nu_i\|_{\Gamma_{i,j}}\big) + \sum_j \|p - \mathcal{P}_H p\|_{-1/2,\Gamma_{i,j}}\|K\nabla\varphi\cdot\nu_i\|_{1/2,\Gamma_{i,j}} \\
&\quad \le CH^{s+1/2}\|p\|_{s+1/2,\Omega_i}\|\varphi\|_{2,\Omega_i}, \quad 0 < s \le m+1,
\end{aligned}
\tag{4.15}
$$

using (3.5), (3.18), (3.14), and (3.10). The proof of (4.10) is completed by Theorem 4.1 and (3.8). Finally, (4.11) follows from (4.10) and (3.6). ◻

**4.3. *A priori* estimates for the mortar pressure.** Let $\|\cdot\|_{d_H}$ be the seminorm induced by $d_H(\cdot,\cdot)$ on $L^2(\Gamma)$, which is

$$
\|\mu\|_{d_H} = d_H(\mu,\mu)^{1/2}, \quad \mu \in L^2(\Gamma).
$$

THEOREM 4.4. *For the mortar pressure $\lambda_H$ of the mixed method* (2.6)–(2.8)*, if* (2.5) *holds, then there exists a positive constant $C$, independent of $h$ and $H$, such that*

$$
\|p - \lambda_H\|_{d_H} \le C\Big\{\sum_{i=1}^n \big(\|p\|_{r+1,\Omega_i} + \|\mathbf{u}\|_{r,\Omega_i}\big)h^r + \|\mathbf{u}-\mathbf{u}_h\|\Big\}, \quad 1 \le r \le k+1.
\tag{4.16}
$$

*In the case of diagonal tensor $K$ and* RTN *spaces on rectangular type grids,*

$$\|p - \lambda_H\|_{d_H} \le C\left\{ \sum_{i=1}^{n} \|\mathbf{u}\|_{r+1,\Omega_i} h^{r+1} + |||\mathbf{u} - \mathbf{u}_h||| \right\}, \quad 0 \le r \le k+1. \tag{4.17}$$

*Proof.* For $\mu \in L^2(\Gamma)$, let

$$\mathbf{u}_h(\mu) = \mathbf{u}_h^*(\mu) + \bar{\mathbf{u}}_h, \quad p_h(\mu) = p_h^*(\mu) + \bar{p}_h,$$

and note that $(\mathbf{u}_h(\mu), p_h(\mu)) \in \mathbf{V}_h \times W_h$ satisfies

$$\begin{aligned} (K^{-1}\mathbf{u}_h(\mu), \mathbf{v})_{\Omega_i} &= (p_h(\mu), \nabla\cdot\mathbf{v})_{\Omega_i} - \langle \mu, \mathbf{v}\cdot\nu\rangle_{\Gamma_i} \\ &\quad - \langle g, \mathbf{v}\cdot\nu\rangle_{\partial\Omega_i\setminus\Gamma}, \qquad \mathbf{v} \in \mathbf{V}_{h,i}, \end{aligned} \tag{4.18}$$

$$(\nabla\cdot\mathbf{u}_h(\mu), w)_{\Omega_i} = (f, w)_{\Omega_i}, \qquad w \in W_{h,i}. \tag{4.19}$$

In particular, $\mathbf{u}_h(\lambda_H) = \mathbf{u}_h$ and $p_h(\lambda_H) = p_h$. Since $\mathbf{u}_h^*(\cdot)$ is linear, (2.15) implies that

$$\begin{aligned} \|p - \lambda_H\|_{d_H} &\le C\|\mathbf{u}_h^*(p) - \mathbf{u}_h^*(\lambda_H)\| = C\|\mathbf{u}_h(p) - \mathbf{u}_h(\lambda_H)\| \\ &= C\|\mathbf{u}_h(p) - \mathbf{u}_h\| \le C\big(\|\mathbf{u}_h(p) - \mathbf{u}\| + \|\mathbf{u} - \mathbf{u}_h\|\big). \end{aligned} \tag{4.20}$$

Bound (4.16) now follows from Theorem 4.1 and the standard mixed method estimate for (2.1)–(2.2) and (4.18)–(4.19) [42, 39, 21]

$$\|\mathbf{u}_h(p) - \mathbf{u}\|_{\Omega_i} \le C(\|p\|_{r+1,\Omega_i} + \|\mathbf{u}\|_{r,\Omega_i})h^r, \quad 1 \le r \le k+1.$$

To show (4.17), we modify (4.20) as

$$\begin{aligned} \|\mathbf{u}_h(p) - \mathbf{u}_h\| &\le \|\mathbf{u}_h(p) - \Pi\mathbf{u}\| + \|\Pi\mathbf{u} - \mathbf{u}_h\| \\ &= \|\mathbf{u}_h(p) - \Pi\mathbf{u}\| + |||\Pi\mathbf{u} - \mathbf{u}_h||| \\ &\le \|\mathbf{u}_h(p) - \Pi\mathbf{u}\| + |||\Pi\mathbf{u} - \mathbf{u}||| + |||\mathbf{u} - \mathbf{u}_h|||, \end{aligned} \tag{4.21}$$

and we apply the superconvergence estimate for $\Pi$ (4.8) and a superconvergence estimate for the standard mixed method

$$\|\mathbf{u}_h(p) - \Pi_i\mathbf{u}\|_{\Omega_i} \le C\|\mathbf{u}\|_{r+1,\Omega_i} h^{r+1}, \quad 0 \le r \le k+1$$

(see [22] and also [36, 24]). ∎

**5. *A posteriori* estimates.** We next derive several *a posteriori* error bounds, which depend only on the input data and the computed solution. The error estimators are utilized in an adaptive mesh refinement procedure to obtain the numerical solution on appropriate subdomain and mortar grids in the next section (see §6.5).

In this section we assume full $H^2$-regularity of the problem (1.1)–(1.3). We want to derive *a posteriori* estimates of the error functions

$$\xi = \mathbf{u} - \mathbf{u}_h, \quad \eta = p - p_h, \quad \text{and} \quad \delta = \lambda - \lambda_H. \tag{5.1}$$

**5.1. Some saturation assumptions.** It is shown in [46, 38] for $\mathrm{RTN}_0$ $(k = 0)$ rectangular elements with linear mortars and very general hanging interface nodes and mortar grid configurations satisfying (2.5) that

$$\sum_{\tau \in \mathcal{T}^{\Gamma,H}} \|\mu\|^2_{1/2,\tau} \le C d_H(\mu,\mu), \quad \mu \in M_H. \tag{5.2}$$

The proofs in [46, 38] can be generalized in a relatively straightforward way to the other mixed finite element spaces under consideration and to higher order elements.

The *a priori* error bounds from Theorems 4.1 and 4.4 motivate the following assumption on the mortar error.

SATURATION ASSUMPTION 1. *There exist a constant* $C$ *such that*

$$|||\lambda - \lambda_H||| := \Bigg( \sum_{\tau \in \mathcal{T}^{\Gamma,H}} \sum_{E \in E_\tau} h_E^{-1} \|\lambda - \lambda_H\|^2_{\partial E \cap \tau} \Bigg)^{1/2} \le C\|\mathbf{u} - \mathbf{u}_h\|. \tag{5.3}$$

For justification of (5.3), note that $|||\lambda - \lambda_H|||$ is closely related to the discrete $H^{1/2}(\Gamma)$ norm and, by (5.2), to $\|\lambda - \lambda_H\|_{d_H}$. Now, assuming that

$$\|\mathbf{u} - \mathbf{u}_h(\lambda)\| \le \gamma \|\mathbf{u} - \mathbf{u}_h\|,$$

which is reasonable, since $\mathbf{u}_h(\lambda)$ is the numerical solution based on the true interface data, we have, using (2.15),

$$\begin{aligned} C\|\lambda - \lambda_H\|_{d_H} &\le \|\mathbf{u}_h^*(\lambda) - \mathbf{u}_h^*(\lambda_H)\| = \|\mathbf{u}_h(\lambda) - \mathbf{u}_h(\lambda_H)\| = \|\mathbf{u}_h(\lambda) - \mathbf{u}_h\| \\ &\le \|\mathbf{u} - \mathbf{u}_h(\lambda)\| + \|\mathbf{u} - \mathbf{u}_h\| \le (1+\gamma)\|\mathbf{u} - \mathbf{u}_h\|. \end{aligned}$$

Let $\mathbf{V}_h'$, $W_h'$, and $M_H'$ be the finite element spaces of index one higher (i.e., of approximation order one more) than $\mathbf{V}_h$, $W_h$, and $M_H$, respectively. Let $\mathbf{u}_h' \in \mathbf{V}_h'$, $p_h' \in W_h'$, and $\lambda_H' \in M_H'$ be the mortar mixed finite element solution in these higher-order spaces (see (2.6)–(2.8)). The *a priori* error estimates from Theorems 4.1 and 4.3 motivate the following assumption.

SATURATION ASSUMPTION 2. *There exist constants* $\beta < 1$, $\beta_{\mathrm{div}} < 1$, *and* $C < \infty$ *such that*

$$\|\mathbf{u} - \mathbf{u}_h'\| \le \beta \|\mathbf{u} - \mathbf{u}_h\|, \tag{5.4}$$

$$\|\nabla \cdot (\mathbf{u} - \mathbf{u}_h')\| \le \beta_{\mathrm{div}} \|\nabla \cdot (\mathbf{u} - \mathbf{u}_h)\|, \tag{5.5}$$

$$\|p - p_h'\| \le C\|p - p_h\|. \tag{5.6}$$

**5.2. Explicit residual-based estimators.** We proceed in this subsection with the derivation of explicit residual-based upper and lower bounds on the error.

**5.2.1. Upper bounds.** Denote, for all $E \in \mathcal{T}_h$, $\tau \in \mathcal{T}^{\Gamma,H}$,

$$\omega_E^2 = \|K^{-1}\mathbf{u}_h + \nabla p_h\|_E^2 h_E^2 + \|f - \nabla \cdot \mathbf{u}_h\|_E^2 h_E^2 + \|\lambda_H - p_h\|^2_{\partial E \cap \Gamma} h_E, \tag{5.7}$$

$$\omega_\tau^2 = \sum_{E \in E_\tau} \|[\mathbf{u}_h \cdot \nu]\|^2_{\partial E \cap \tau} H_\tau^3, \tag{5.8}$$

where for any $\mathbf{v} \in \mathbf{V}$, $\mathbf{v}|_{\Omega_i} = \mathbf{v}_i$,

$$[\mathbf{v} \cdot \nu]|_{\Gamma_{i,j}} = \mathbf{v}_i \cdot \nu_i + \mathbf{v}_j \cdot \nu_j$$

is the jump operator. We have an upper bound on the pressure error $\eta$.

THEOREM 5.1. *There exists a constant $C$, independent of $h$ and $H$, such that*

$$\|\eta\|^2 \leq C\Big\{ \sum_{E\in\mathcal{T}_h} \omega_E^2 + \sum_{\tau\in\mathcal{T}^{\Gamma,H}} \omega_\tau^2 + \sum_{e\in\mathcal{T}_h|_{\partial\Omega}} \|g - \mathcal{Q}_h g\|_e^2 h_e \Big\}. \tag{5.9}$$

Note that $\mathcal{Q}_h$ is applied on $\partial\Omega$, where it is single valued. The proof of this theorem follows closely the proof of Theorem 3.1 in [44] with a straightforward modification of the argument to allow for the two scales $h$ and $H$.

REMARK 5.1. Due to the approximation property (3.9) of $\mathcal{Q}_h$, the last term in the bound of Theorem 5.1 is of higher order than the other terms. Therefore its effect becomes negligible for small $h$.

The bound on $\xi$ is expressed in terms of $h_E^{-1}\omega_E$ and $H_\tau^{-1}\omega_\tau$.

THEOREM 5.2. *Assume that the saturation assumptions* (5.3), (5.4), *and* (5.6) *hold. Then there exist a constant $C$, independent of $\beta$, $h$, and $H$, such that*

$$\|\xi\|_{H(\mathrm{div};\Omega)}^2 \leq \frac{C}{(1-\beta)^2}\Big\{ \sum_{E\in\mathcal{T}_h} h_E^{-2}\omega_E^2 + \sum_{\tau\in\mathcal{T}^{\Gamma,H}} H_\tau^{-2}\omega_\tau^2 + \sum_{e\in\mathcal{T}_h|_{\partial\Omega}} \|g - \mathcal{Q}_h g\|_e^2 h_e^{-1} \Big\}.$$

The proof of this theorem follows closely the proof of Theorem 3.2 in [44] with a straightforward modification of the argument to allow for the two scales $h$ and $H$.

**5.2.2. Lower bounds.** Next, we establish lower bounds on the error, which indicate that the residual error estimators can be used effectively in an adaptive mesh refinement algorithm.

THEOREM 5.3. *There exists a constant $C$, independent of $h$ and $H$, such that*

$$\begin{aligned} \sum_{E\in\mathcal{T}_h} \omega_E^2 + \sum_{\tau\in\mathcal{T}^{\Gamma,H}} \omega_\tau^2 \leq C\Big\{ \|\eta\|^2 &+ \sum_{E\in\mathcal{T}_h} h_E^2 \|\xi\|_{H(\mathrm{div};E)}^2 + \sum_{E\in\mathcal{T}_h} h_E \|\delta\|_{\partial E\cap\Gamma}^2 \\ &+ \sum_{\tau\in\mathcal{T}^{\Gamma,H}} \sum_{E\in E_\tau} h_E^{-1} H_\tau^3 \|\xi\|_{H(\mathrm{div};E)}^2 \Big\}. \end{aligned} \tag{5.10}$$

*Moreover, the following local bounds hold for any $E \in \mathcal{T}_h$, $e \in \partial E$, and $\tau \in \mathcal{T}^{\Gamma,H}$:*

$$\|K^{-1}\mathbf{u}_h + \nabla p_h\|_E^2 h_E^2 + \|f - \nabla\cdot\mathbf{u}_h\|_E^2 h_E^2 \leq C(\|\eta\|_E^2 + \|\xi\|_{H(\mathrm{div};E)}^2 h_E^2), \tag{5.11}$$

$$\sum_{E\in E_\tau} \|[\mathbf{u}_h \cdot \nu]\|_{\partial E\cap\tau}^2 H_\tau^3 \leq C \sum_{E\in E_\tau} h_E^{-1} H_\tau^3 \|\xi\|_{H(\mathrm{div};E)}^2, \tag{5.12}$$

$$\|\lambda_H - p_h\|_e^2 h_E \leq C(\|\eta\|_E^2 + \|\xi\|_{H(\mathrm{div};E)}^2 h_E^2 + \|\delta\|_e^2 h_E). \tag{5.13}$$

The proof is a relatively straightforward modification of the proof of Theorem 3.3 in [44].

REMARK 5.2. Generally, the terms after $\|\eta\|^2$ in (5.10) are of higher order. From Remarks 4.1 and 4.3, when $l = k$, the choice $H = \mathcal{O}(h^{(k+1)/(m+1/2)})$ gives optimal *a priori* errors of order $\mathcal{O}(h^{k+1})$ for $p$ in $L^2$ and $\mathbf{u}$ in $H(\mathrm{div};\Omega)$, as well as for the mortar

$\lambda = p$ in the $d_H$-norm (which bounds the $L^2$-norm). Thus for $C_1$ and $C_2$ independent of $h$,

$$C_1\Big( \sum_{E\in\mathcal{T}_h} \omega_E^2 + \sum_{\tau\in\mathcal{T}^{\Gamma,H}} \omega_\tau^2 + \mathcal{O}(h^{2(k+1)+\alpha})\Big) \le \|\eta\|^2 \le C_2\Big( \sum_{E\in\mathcal{T}_h} \omega_E^2 + \sum_{\tau\in\mathcal{T}^{\Gamma,H}} \omega_\tau^2 + \mathcal{O}(h^{2(k+1)+1})\Big), \tag{5.14}$$

where $\alpha = \min\big(1, 3(k+1)/(m+1/2)-1\big)$. In the case of $\mathrm{RTN}_0$ ($k=0$) and quadratic mortars ($m=2$), the optimal choice is $H = \mathcal{O}(h^{2/5})$, and $\alpha = 1/5 > 0$. Similarly, for linear mortars ($m = 1$) with $H = \mathcal{O}(h^{2/3})$, $\alpha = 1 > 0$. Whenever $\alpha > 0$, the error in $\|\eta\|^2$ is dominated above and below by our local residual estimators $\sum_{E\in\mathcal{T}_h} \omega_E^2 + \sum_{\tau\in\mathcal{T}^{\Gamma,H}} \omega_\tau^2$ for small enough $h$, up to $C_1$ and $C_2$, and so this quantity is an efficient and reliable indicator of the pressure error.

**5.3. Error estimators based on solving local problems.** In this subsection we develop an implicit error estimator which requires solving local (element) boundary value problems. These problems approximate the local residual equations satisfied by the true error. The motivation for considering implicit estimators comes from the unknown generic constants that appear in the explicit estimators. We show that the implicit estimator provides both optimal upper and lower bounds for the velocity error.

**5.3.1. Global approximation to the error.** Following the approach in [45], we first construct a global approximation to the error based on higher order finite element spaces. For $\mathbf{v} \in \mathbf{V}_i$, let

$$r(\mathbf{v}) = -\langle g, \mathbf{v}\cdot\nu\rangle_{\partial\Omega_i\setminus\Gamma} - (K^{-1}\mathbf{u}_h, \mathbf{v})_{\Omega_i} + (p_h, \nabla\cdot\mathbf{v})_{\Omega_i} - \langle \lambda_H, \mathbf{v}\cdot\nu_i\rangle_{\Gamma_i}. \tag{5.15}$$

Using (2.1)–(2.3), the true error satisfies the residual equations

$$(K^{-1}\xi, \mathbf{v})_{\Omega_i} - (\eta, \nabla\cdot\mathbf{v})_{\Omega_i} + \langle \delta, \mathbf{v}\cdot\nu_i\rangle_{\Gamma_i} = r(\mathbf{v}), \quad \mathbf{v}\in\mathbf{V}_i, \tag{5.16}$$

$$(\nabla\cdot\xi, w)_{\Omega_i} = (f - \nabla\cdot\mathbf{u}_h, w)_{\Omega_i}, \quad w \in W_i, \tag{5.17}$$

$$\sum_{i=1}^n \langle \xi\cdot\nu_i, \mu\rangle_{\Gamma_i} = -\sum_{i=1}^n \langle \mathbf{u}_h\cdot\nu_i, \mu\rangle_{\Gamma_i}, \quad \mu\in M. \tag{5.18}$$

Recall from the previous subsection that $\mathbf{V}_h' \times W_h' \times M_H'$ is the mortar mixed finite element space of index order one higher than $\mathbf{V}_h \times W_h \times M_H$. Let

$$\xi' = \mathbf{u}_h' - \mathbf{u}_h, \quad \eta' = p_h' - p_h, \quad \text{and} \quad \delta' = \lambda_H' - \lambda_H. \tag{5.19}$$

Then $(\xi', \eta', \delta') \in \mathbf{V}_h' \times W_h' \times M_H'$ is the finite element approximation to $(\xi, \eta, \delta)$ satisfying

$$(K^{-1}\xi', \mathbf{v})_{\Omega_i} - (\eta', \nabla\cdot\mathbf{v})_{\Omega_i} + \langle \delta', \mathbf{v}\cdot\nu_i\rangle_{\Gamma_i} = r(\mathbf{v}), \quad \mathbf{v}\in\mathbf{V}_{h,i}', \tag{5.20}$$

$$(\nabla\cdot\xi', w)_{\Omega_i} = (f - \nabla\cdot\mathbf{u}_h, w)_{\Omega_i}, \quad w \in W_{h,i}', \tag{5.21}$$

$$\sum_{i=1}^n \langle \xi'\cdot\nu_i, \mu\rangle_{\Gamma_i} = -\sum_{i=1}^n \langle \mathbf{u}_h\cdot\nu_i, \mu\rangle_{\Gamma_i}, \quad \mu\in M_H'. \tag{5.22}$$

The saturation assumptions (5.4) and (5.5) imply

$$\frac{1}{1+\beta}\|\xi'\| \leq \|\xi\| \leq \frac{1}{1-\beta}\|\xi'\|, \tag{5.23}$$

$$\frac{1}{1+\beta_{\text{div}}}\|\nabla\cdot\xi'\| \leq \|\nabla\cdot\xi\| \leq \frac{1}{1-\beta_{\text{div}}}\|\nabla\cdot\xi'\|, \tag{5.24}$$

so it is enough to estimate $\xi'$, since we do not wish to compute $\mathbf{u}'_h$.

**5.3.2. Local (element) approximation to the error.** For any $E \in \mathcal{T}_h$, the true error satisfies the local equations

$$(K^{-1}\xi, \mathbf{v})_E - (\eta, \nabla\cdot\mathbf{v})_E = r_E(\mathbf{v}) - \langle p, \mathbf{v}\cdot\nu_E\rangle_{\partial E}, \quad \mathbf{v} \in \mathbf{V}(E), \tag{5.25}$$

$$(\nabla\cdot\xi, w)_E = (f - \nabla\cdot\mathbf{u}_h, w)_E, \quad w \in W(E), \tag{5.26}$$

where

$$r_E(\mathbf{v}) = -(K^{-1}\mathbf{u}_h, \mathbf{v})_E + (p_h, \nabla\cdot\mathbf{v})_E. \tag{5.27}$$

We construct a higher order local approximation of the error by solving element subproblems: Find $\psi' \in \mathbf{V}'_h(E)$ and $\theta' \in W'_h(E)$ such that

$$(K^{-1}\psi', \mathbf{v})_E - (\theta', \nabla\cdot\mathbf{v})_E = r_E(\mathbf{v}) - \langle p_A, \mathbf{v}\cdot\nu_E\rangle_{\partial E}, \quad \mathbf{v} \in \mathbf{V}'_h(E), \tag{5.28}$$

$$(\nabla\cdot\psi', w)_E = (f - \nabla\cdot\mathbf{u}_h, w)_E, \quad w \in W'_h(E). \tag{5.29}$$

where $p_A = g$ on $\partial\Omega$, $p_A = \lambda_H$ on $\partial E \cap \Gamma$, and $p_A = \tilde{p}_h$ on $\partial E \cap \mathcal{E}_h$, where $\tilde{p}_h \in \Lambda_h(\partial E) = \mathbf{V}_h(E)\cdot\nu$ is the Lagrange multiplier for $\mathbf{V}_h$ and $W_h$ in the standard hybrid formulation of the mixed method [10, 16], which can be defined from $\mathbf{u}_h$ and $p_h$ as

$$\langle \tilde{p}_h, \mathbf{v}\cdot\nu_E\rangle_{\partial E} = -(K^{-1}\mathbf{u}_h, \mathbf{v})_E + (p_h, \nabla\cdot\mathbf{v})_E, \quad \mathbf{v} \in \mathbf{V}_h(E). \tag{5.30}$$

Note that (2.6) implies that $\tilde{p}_h$ is single-valued on $\mathcal{E}_h$. Let $\tilde{p}'$ be the Lagrange multiplier for the higher order spaces $\mathbf{V}'_h$ and $W'_h$ satisfying

$$\langle \tilde{p}', \mathbf{v}\cdot\nu_E\rangle_{\partial E} = -(K^{-1}\mathbf{u}'_h, \mathbf{v})_E + (p'_h, \nabla\cdot\mathbf{v})_E, \quad \mathbf{v} \in V'_h(E). \tag{5.31}$$

Again, $\tilde{p}'$ is single-valued on $\mathcal{E}_h$.

We need one last saturation assumption.

SATURATION ASSUMPTION 3. *There exist a constant $C$ such that*

$$\left(\sum_{e\in\mathcal{E}_h} h_e^{-1}\|\tilde{p}' - \tilde{p}_h\|_e^2\right)^{1/2} \leq C\|\mathbf{u} - \mathbf{u}_h\|. \tag{5.32}$$

The assumption (5.32) is motivated by the *a priori* error estimate for the Lagrange multiplier [16]

$$\left(\sum_{e\in\mathcal{E}_h} h_e^{-1}\|\bar{p} - \tilde{p}_h\|_e^2\right)^{1/2} \leq Ch^{k+1},$$

where $\bar{p}$ is the $L^2$-projection of $p$ onto $\mathbf{V}_h\cdot\nu|_{\mathcal{E}_h}$.

THEOREM 5.4. *If the saturation assumptions* (5.3), (5.4), (5.5), *and* (5.32) *hold, then there exist constants* $C_1$ *and* $C_2$, *independent of* $\beta$ *and* $\beta_{\rm div}$, *such that*

$$C_1\left[\|\psi'\|_{H(\mathrm{div};\Omega)} + \left(\sum_{\tau\in\mathcal{T}^{\Gamma,H}}\sum_{E\in E_\tau}\|[\mathbf{u}_h\cdot\nu]\|^2_{\partial E\cap\tau}h_E\right)^{1/2}\right] \le \|\xi\|_{H(\mathrm{div};\Omega)} \tag{5.33}$$
$$\le \frac{C_2}{(1-\beta_{max})^2}\left[\|\psi'\|_{H(\mathrm{div};\Omega)} + \left(\sum_{\tau\in\mathcal{T}^{\Gamma,H}}\sum_{E\in E_\tau}\|[\mathbf{u}_h\cdot\nu]\|^2_{\partial E\cap\tau}h_E\right)^{1/2}\right],$$

*where* $\beta_{max} = \max\{\beta,\beta_{\rm div}\}$.

The proof is similar to the proof of Theorem 4.1 in [44], but differs in the technical details in handling the two scales. We reproduce the proof here for completeness.

*Proof.* Due to (5.21) and (5.29), it holds on every $E\in\mathcal{T}_h$ that

$$\nabla\cdot\psi' = \nabla\cdot\xi'. \tag{5.34}$$

Next, the sum over all elements in (5.28) with $\mathbf{v} = \psi'-\xi'$ gives

(5.35)
$$\begin{aligned}
&\sum_{E\in\mathcal{T}_h}\big[(K^{-1}(\psi'-\xi'),\psi'-\xi')_E - (\theta'-\eta',\nabla\cdot(\psi'-\xi'))_E\big]\\
&\quad= \sum_{E\in\mathcal{T}_h}\big[-(K^{-1}\xi',\psi'-\xi')_E + (\eta',\nabla\cdot(\psi'-\xi'))_E\\
&\qquad\qquad + r_E(\psi'-\xi') - \langle p_A,(\psi'-\xi')\cdot\nu_E\rangle_{\partial E}\big]\\
&\quad= \sum_{E\in\mathcal{T}_h}\big[-(K^{-1}\mathbf{u}_h',\psi'-\xi')_E + (p_h',\nabla\cdot(\psi'-\xi'))_E - \langle\tilde p_h,(\psi'-\xi')\cdot\nu_E\rangle_{\partial E\cap\mathcal{E}_h}\\
&\qquad\qquad - \langle g,(\psi'-\xi')\cdot\nu\rangle_{\partial E\cap\partial\Omega} - \langle\lambda_H,(\psi'-\xi')\cdot\nu_E\rangle_{\partial E\cap\Gamma}\big]\\
&\quad= \sum_{E\in\mathcal{T}_h}\big[\langle\tilde p'-\tilde p_h,(\psi'-\xi')\cdot\nu_E\rangle_{\partial E\cap\mathcal{E}_h} + \langle\lambda_H'-\lambda_H,(\psi'-\xi')\cdot\nu_E\rangle_{\partial E\cap\Gamma}\big],
\end{aligned}$$

wherein for the last equality we have used (5.31) and (2.6) for the higher order (primed) spaces to see that $\tilde p'$ is the projection of $g$ on $\partial\Omega$ and the projection of $\lambda_H'$ on $\Gamma$. The first term on the right can be bounded as

$$\begin{aligned}
&\left|\sum_{E\in\mathcal{T}_h}\langle\tilde p'-\tilde p_h,(\psi'-\xi')\cdot\nu_E\rangle_{\partial E\cap\mathcal{E}_h}\right|\\
&\qquad\le \sum_{e\in\mathcal{E}_h}h_e^{-1/2}\|\tilde p'-\tilde p_h\|_e h_e^{1/2}\|(\psi'-\xi')\cdot\nu_e\|_e\\
&\qquad\le C\|\xi\|\|\psi'-\xi'\|.
\end{aligned} \tag{5.36}$$

using the saturation assumption (5.32) and the well known local trace inequality akin to (3.18)

$$\forall\,E\in\mathcal{T}_h,\ e\in\partial E,\quad \|\mathbf{v}\cdot\nu\|_e \le Ch_E^{-1/2}\|\mathbf{v}\|_E,\quad \forall\,\mathbf{v}\in\mathbf{V}_h. \tag{5.37}$$

For the second term on the right in (5.35) we have

$$\left|\sum_{E\in\mathcal{T}_h}\langle\lambda_H'-\lambda_H,(\psi'-\xi')\cdot\nu_E\rangle_{\partial E\cap\Gamma}\right|=\left|\sum_{i=1}^{n}\langle\delta',(\psi'-\xi')\cdot\nu_i\rangle_{\Gamma_i}\right| \tag{5.38}$$
$$\le\sum_{\tau\in\mathcal{T}^{\Gamma,h}}\sum_{E\in E_\tau}h_E^{-1/2}\|\delta'\|_{\partial E\cap\tau}h_E^{1/2}\|[(\psi'-\xi')\cdot\nu]\|_{\partial E\cap\tau}$$
$$\le|||\delta'|||\,\|\psi'-\xi'\|$$
$$\le C\|\xi\|\|\psi'-\xi'\|,$$

where we have used (5.37), (5.3), and (5.4) in the last two inequalities.

A combination of (5.34)–(5.38) implies that

$$\|\psi'-\xi'\|\le C\|\xi\|,$$

and therefore

$$\|\psi'\|\le C\|\xi\|, \tag{5.39}$$

using (5.23). The divergence bound

$$\|\nabla\cdot\psi'\|\le\|\nabla\cdot\xi\|$$

follows from (5.29) with $w=\nabla\cdot\psi'$, since $f-\nabla\cdot\mathbf{u}_h=\nabla\cdot\xi$. Therefore

$$\|\psi'\|_{H(\mathrm{div};\Omega)}\le C\|\xi\|_{H(\mathrm{div};\Omega)}. \tag{5.40}$$

This with (5.12) completes the proof of the left inequality in (5.33).

For the right inequality in (5.33), from (5.35), we have (with (5.34)) that

$$\begin{aligned}(5.41)\quad&(K^{-1}(\psi'-\xi'),\psi'-\xi')\\&=\sum_{E\in\mathcal{T}_h}\big[\langle\tilde p'-\tilde p_h,(\psi'-\xi')\cdot\nu_E\rangle_{\partial E\cap\mathcal{E}_h}+\langle\lambda_H'-\lambda_H,(\psi'-\xi')\cdot\nu_E\rangle_{\partial E\cap\Gamma}\big]\\&=-\sum_{i}\langle\delta',\xi'\cdot\nu_i\rangle_{\Gamma_i}-\sum_{E\in\mathcal{T}_h}\big[\langle\tilde p'-\tilde p_h,\psi'\cdot\nu_E\rangle_{\partial E\cap\mathcal{E}_h}+\langle\lambda_H'-\lambda_H,\psi'\cdot\nu_E\rangle_{\partial E\cap\Gamma}\big].\end{aligned}$$

Using (5.22), for any $\epsilon>0$, the first term on the right can be bounded as

$$\left|\sum_{i=1}^{n}\langle\delta',\xi'\cdot\nu_i\rangle_{\Gamma_i}\right|=\left|\sum_{i=1}^{n}\langle\delta',\mathbf{u}_h\cdot\nu_i\rangle_{\Gamma_i}\right| \tag{5.42}$$
$$\le\sum_{\tau\in\mathcal{T}^{\Gamma,h}}\sum_{E\in E_\tau}h_E^{-1/2}\|\delta'\|_{\partial E\cap\tau}h_E^{1/2}\|[\mathbf{u}_h\cdot\nu]\|_{\partial E\cap\tau}$$
$$\le\epsilon\|\xi\|^2+C\epsilon^{-1}\sum_{\tau\in\mathcal{T}^{\Gamma,h}}\sum_{E\in E_\tau}\|[\mathbf{u}_h\cdot\nu]\|^2_{\partial E\cap\tau}h_E,$$

where we have used (5.3) and (5.4) in the last inequality. For the last two terms on the right in (5.41), arguments similar to (5.36) and (5.38) give

$$\left|\sum_{E\in\mathcal{T}_h}\big[\langle\tilde p'-\tilde p_h,\psi'\cdot\nu_E\rangle_{\partial E\cap\mathcal{E}_h}+\langle\lambda_H'-\lambda_H,\psi'\cdot\nu_E\rangle_{\partial E\cap\Gamma}\big]\right| \tag{5.43}$$
$$\le\epsilon\|\xi\|^2+C\epsilon^{-1}\|\psi'\|^2.$$

Combining (5.41)–(5.43), using the triangle inequality and (5.23), and taking $\epsilon$ proportional to $(1-\beta)^2$, we obtain

$$\|\xi\| \le \frac{C}{(1-\beta)^2}\left[\|\psi'\| + \left(\sum_{\tau\in\mathcal{T}^{\Gamma,h}}\sum_{E\in E_\tau}\|[\mathbf{u}_h\cdot\nu]\|^2_{\partial E\cap\tau}h_E\right)^{1/2}\right].$$

An application of (5.24) and (5.34) completes the proof. ∎

**6. Numerical results.** In this section we present several numerical tests confirming the theoretical convergence rates and illustrating the behavior of the method. The examples are on the unit square (cube for Example 3), and use the lowest order Raviart-Thomas-Nedelec spaces [39, 37], $\mathrm{RTN}_0$, on rectangles (for which $k = l = 0$). The boundary conditions are Dirichlet on the left and right edges and Neumann on the rest of the boundary. The domain is divided into four (eight for Example 3) subdomains with interfaces along the $x = 1/2$ and $y = 1/2$ (and $z = 1/2$ for Example 3) lines. We employ the non-overlapping domain decomposition algorithm from Section 2.2 for the solution of the algebraic problem.

The convergence rates are established by running the test case on several levels of grid refinement and computing a least squares fit to the error. We consider both matching and non-matching initial grids. The initial matching grids are $2\times2$ ($2\times2\times2$ for Example 3) and the initial non-matching grids are chosen to be $2\times2$ or $3\times3$ in a checkerboard fashion. We test both continuous and discontinuous quadratic mortars ($m = 2$) and compare the results to the cases of linear mortars ($m = 1$), continuous or discontinuous, respectively. The initial mortar grids on all interfaces have one element. For the case of quadratic mortars, on each level of grid refinement we divide each subdomain element diameter by four and halve each mortar element diameter so that $H = h^{1/2}$ (see Remarks 4.1–4.3). For the case of linear mortars we halve both subdomain and mortar element diameters, so $H = 2h$ on each level.

TABLE 6.1
*Theoretical convergence rates for quadratic and linear mortars.*

| $m$ | $H$ | $\|\|p-p_h\|\|$ | $\|\|\mathbf{u}-\mathbf{u}_h\|\|$ | $\|\|\|p-p_h\|\|\|$ | $\|\|\|\mathbf{u}-\mathbf{u}_h\|\|\|$ | $\|\|\|p-\lambda_H\|\|\|$ | |
|---|---|---|---|---|---|---|---|
| | | | | | | *full K* | *diag K* |
| 2 | $h^{1/2}$ | 1 | 1 | 1.5 | 1.25 | 1.25 | 1.5 |
| 1 | $2h$ | 1 | 1 | 2 | 1.5 | 1.5 | 2 |

The theoretical convergence rates for the above choices of subdomain and mortar grids are given in Table 6.1. The second pressure error in the tables, $|||p-p_h|||$, is the discrete $L^2$-norm induced by the midpoint rule on $\mathcal{T}_h$, which is $\mathcal{O}(h^2)$-close to $\|\hat{p}-p_h\|$. The discrete velocity error $|||\mathbf{u}-\mathbf{u}_h|||$ is defined in (4.6) above. The discrete interface pressure error $|||p-\lambda_H|||$ is computed by adding for each block $\Omega_i$ the discrete $L^2$-norm of $p-\mathcal{Q}_{h,i}\lambda_H$ induced by the midpoint rule on the traces of $\mathcal{T}_{h,i}$ on $\partial\Omega_i\cap\Gamma$. This is essentially the $L^2$-norm, and we expect it to be 1/2 power of $H$ better than $\|p-\lambda_H\|_{d_H}$, since the latter is essentially $\|p-\lambda_H\|_{H^{1/2}(\Gamma)}$ (see [20], [46], and Remark 6.1 in [5]).

**6.1. Example 1.** In the first example we solve a problem with known analytic solution

$$p(x,y) = x^3y^4 + x^2 + \sin(xy)\cos(y)$$

and full tensor coefficient

$$K = \begin{pmatrix} (x+1)^2 + y^2 & \sin(xy) \\ \sin(xy) & (x+1)^2 \end{pmatrix}.$$

Convergence rates for this test case are given in Tables 6.2–6.5. We also report the number of interface iterations needed for convergence of the domain decomposition solver and the condition number of the interface operator. We observe that the convergence rates are at least as good as predicted by the theory. For all four cases we obtain optimal order $\mathcal{O}(h)$ for both the pressure and the velocity $L^2$-error.

The discrete pressure error $|||p - p_h||| \approx \|\hat{p} - p_h\|$ is superconvergent of order $\mathcal{O}(h^2)$ for both quadratic and linear mortars, even though Theorem 4.3 predicts only $\mathcal{O}(h^{3/2})$ for quadratic mortars. By Theorem 4.2, the discrete velocity error $|||\mathbf{u}-\mathbf{u}_h|||$ is superconvergent of order $\mathcal{O}(h^{5/4})$ for quadratic mortars and $\mathcal{O}(h^{3/2})$ for linear mortars. Again, we observe higher than expected superconvergence for the case of quadratic mortars. Lastly, the discrete interface pressure error $|||p-\lambda_H||| \approx H^{1/2}\|p-\lambda_H\|_{d_H}$ is also better than expected, achieving convergence of $\mathcal{O}(h^2)$.

Table 6.2

*Number of iterations, condition number, discrete norm errors and convergence rates for Example 1: continuous quadratic mortars and matching grids.*

| $1/h$ | *iter.* | *cond.* | $\|\|p - p_h\|\|$ | $\|\|\mathbf{u} - \mathbf{u}_h\|\|$ | $\|\|\|p - p_h\|\|\|$ | $\|\|\|\mathbf{u} - \mathbf{u}_h\|\|\|$ | $\|\|\|p - \lambda_H\|\|\|$ |
|---|---|---|---|---|---|---|---|
| 4 | 8 | 5.46E+0 | 3.38E-1 | 3.00E-1 | 6.87E-2 | 2.13E-2 | 5.81E-2 |
| 16 | 15 | 1.87E+1 | 7.98E-2 | 6.93E-2 | 4.21E-3 | 1.89E-3 | 3.50E-3 |
| 64 | 22 | 6.02E+1 | 1.99E-2 | 1.72E-2 | 2.59E-4 | 1.97E-4 | 2.17E-4 |
| 256 | 33 | 1.74E+2 | 4.97E-3 | 4.31E-3 | 1.62E-5 | 2.44E-5 | 1.39E-5 |
| rate | | | $\mathcal{O}(h^{1.01})$ | $\mathcal{O}(h^{1.02})$ | $\mathcal{O}(h^{2.01})$ | $\mathcal{O}(h^{1.63})$ | $\mathcal{O}(h^{2.01})$ |

Table 6.3

*Number of iterations, condition number, discrete norm errors and convergence rates for Example 1: continuous linear mortars and matching grids.*

| $1/h$ | *iter.* | *cond.* | $\|\|p - p_h\|\|$ | $\|\|\mathbf{u} - \mathbf{u}_h\|\|$ | $\|\|\|p - p_h\|\|\|$ | $\|\|\|\mathbf{u} - \mathbf{u}_h\|\|\|$ | $\|\|\|p - \lambda_H\|\|\|$ |
|---|---|---|---|---|---|---|---|
| 4 | 8 | 9.07E+0 | 3.38E-1 | 3.00E-1 | 6.87E-2 | 2.13E-2 | 5.81E-2 |
| 8 | 11 | 8.72E+0 | 1.62E-1 | 1.41E-1 | 1.70E-2 | 6.33E-3 | 1.42E-2 |
| 16 | 14 | 1.57E+1 | 7.98E-2 | 6.93E-2 | 4.21E-3 | 1.88E-3 | 3.50E-3 |
| 32 | 18 | 3.08E+1 | 3.98E-2 | 3.45E-2 | 1.04E-3 | 5.88E-4 | 8.67E-4 |
| 64 | 26 | 6.15E+1 | 1.99E-2 | 1.72E-2 | 2.59E-4 | 1.93E-4 | 2.16E-4 |
| 128 | 36 | 1.23E+2 | 9.94E-3 | 8.62E-3 | 6.46E-5 | 6.53E-5 | 5.38E-5 |
| 256 | 50 | 2.46E+2 | 4.97E-3 | 4.31E-3 | 1.62E-5 | 2.28E-5 | 1.36E-5 |
| rate | | | $\mathcal{O}(h^{1.01})$ | $\mathcal{O}(h^{1.02})$ | $\mathcal{O}(h^{2.01})$ | $\mathcal{O}(h^{1.65})$ | $\mathcal{O}(h^{2.01})$ |

Based on comparing the results from linear and quadratic mortars, we observe that for fine meshes the quadratic mortars are more efficient: we achieve the same accuracy with less computational work. For example, for the finest level of grid refinement, the accuracy is comparable but there is more than a 30% reduction in the number of interface problem iterations needed for both continuous and discontinuous quadratic mortars.

The computed pressure and velocity with discontinuous quadratic and linear mortars on the same non-matching subdomain grids (first/second level of refinement for

TABLE 6.4
*Number of iterations, condition number, discrete norm errors and convergence rates for Example 1: discontinuous quadratic mortars and non-matching grids.*

| $1/h$ | *iter.* | *cond.* | $\|\|p-p_h\|\|$ | $\|\|\mathbf{u}-\mathbf{u}_h\|\|$ | $\|\|\|p-p_h\|\|\|$ | $\|\|\|\mathbf{u}-\mathbf{u}_h\|\|\|$ | $\|\|\|p-\lambda_H\|\|\|$ |
|---|---|---|---|---|---|---|---|
| 4 | 12 | 1.69E+1 | 2.64E-1 | 2.03E-1 | 4.62E-2 | 2.13E-2 | 4.45E-2 |
| 16 | 17 | 2.25E+1 | 6.37E-2 | 4.86E-2 | 2.83E-3 | 1.82E-3 | 2.72E-3 |
| 64 | 29 | 6.95E+1 | 1.59E-2 | 1.21E-2 | 1.75E-4 | 1.59E-4 | 1.69E-4 |
| 256 | 48 | 1.91E+2 | 3.98E-3 | 3.03E-3 | 1.09E-5 | 1.69E-5 | 1.07E-5 |
| rate | | | $\mathcal{O}(h^{1.01})$ | $\mathcal{O}(h^{1.01})$ | $\mathcal{O}(h^{2.01})$ | $\mathcal{O}(h^{1.72})$ | $\mathcal{O}(h^{2.01})$ |

TABLE 6.5
*Number of iterations, condition number, discrete norm errors and convergence rates for Example 1: discontinuous linear mortars and non-matching grids.*

| $1/h$ | *iter.* | *cond.* | $\|\|p-p_h\|\|$ | $\|\|\mathbf{u}-\mathbf{u}_h\|\|$ | $\|\|\|p-p_h\|\|\|$ | $\|\|\|\mathbf{u}-\mathbf{u}_h\|\|\|$ | $\|\|\|p-\lambda_H\|\|\|$ |
|---|---|---|---|---|---|---|---|
| 4 | 8 | 6.28E+0 | 2.63E-1 | 2.04E-1 | 4.54E-2 | 2.35E-2 | 4.55E-2 |
| 8 | 13 | 1.24E+1 | 1.28E-1 | 9.82E-2 | 1.14E-2 | 7.44E-3 | 1.14E-2 |
| 16 | 19 | 2.55E+1 | 6.37E-2 | 4.86E-2 | 2.82E-3 | 2.30E-3 | 2.86E-3 |
| 32 | 28 | 5.19E+1 | 3.18E-2 | 2.43E-2 | 7.01E-4 | 7.29E-4 | 7.13E-4 |
| 64 | 41 | 1.05E+2 | 1.59E-2 | 1.21E-2 | 1.75E-4 | 2.38E-4 | 1.78E-4 |
| 128 | 59 | 2.12E+2 | 7.95E-3 | 6.06E-3 | 4.37E-5 | 7.99E-5 | 4.45E-5 |
| 256 | 85 | 4.25E+2 | 3.98E-3 | 3.03E-3 | 1.09E-5 | 2.75E-5 | 1.12E-5 |
| rate | | | $\mathcal{O}(h^{1.01})$ | $\mathcal{O}(h^{1.01})$ | $\mathcal{O}(h^{2.00})$ | $\mathcal{O}(h^{1.63})$ | $\mathcal{O}(h^{2.00})$ |

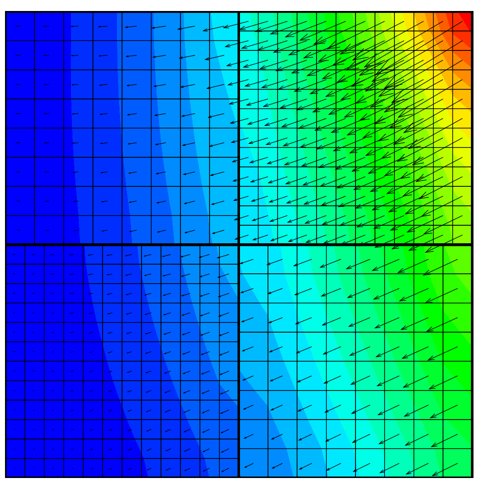

A. *Discontinuous quadratic mortars*

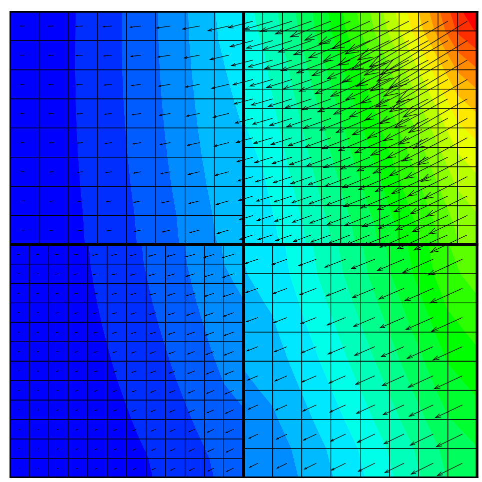

B. *Discontinuous linear mortars*

FIG. 6.1. *Computed pressure (shade) and velocity (arrows) for Example 1 on non-matching grids.*

quadratic/linear mortars) are shown in Figure 6.1. Although the two solutions look the same, the velocity error along the interfaces is somewhat larger for the case of linear mortars, as can be seen in Figure 6.2 where the magnified numerical error is shown.

**6.2. Example 2.** In the second example we test a problem with a discontinuous coefficient. We choose $K = I$ for $0 \le x < 1/2$ and $K = 10I$ for $1/2 < x \le 1$. The

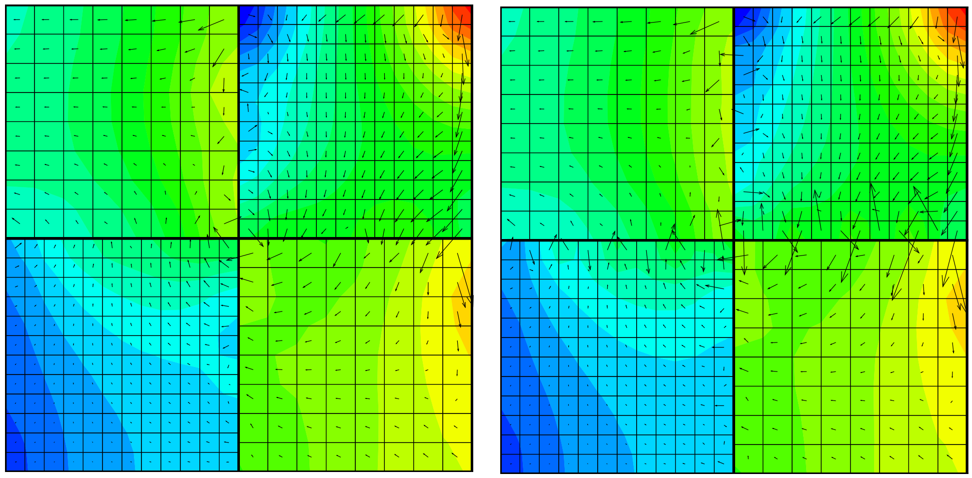

A. *Discontinuous quadratic mortars* B. *Discontinuous linear mortars*

FIG. 6.2. *Error in pressure (shade) and velocity (arrows) for Example 1 on non-matching grids.*

solution

$$p(x,y) = \begin{cases} x^2y^3 + \cos(xy), & 0 \le x \le 1/2, \\ \left(\frac{2x+9}{20}\right)^2 y^3 + \cos\left(\frac{2x+9}{20}y\right), & 1/2 \le x \le 1, \end{cases}$$

is chosen to be continuous and have continuous normal flux at $x = 1/2$. Convergence rates are given in Tables 6.6–6.9. Again they agree with the theory, even though $K$ is mildly discontinuous.

TABLE 6.6
*Number of iterations, condition number, discrete norm errors and convergence rates for Example 2: discontinuous quadratic mortars and matching grids.*

| $1/h$ | *iter.* | *cond.* | $\|\|p-p_h\|\|$ | $\|\|\mathbf{u}-\mathbf{u}_h\|\|$ | $\|\|\|p-p_h\|\|\|$ | $\|\|\|\mathbf{u}-\mathbf{u}_h\|\|\|$ | $\|\|\|p-\lambda_H\|\|\|$ |
|---|---|---|---|---|---|---|---|
| 4 | 8 | 1.45E+1 | 2.35E-2 | 8.17E-2 | 1.51E-3 | 6.77E-2 | 4.58E-3 |
| 16 | 19 | 4.40E+1 | 5.69E-3 | 1.95E-2 | 1.07E-4 | 4.46E-3 | 2.98E-4 |
| 64 | 38 | 1.30E+2 | 1.42E-3 | 4.87E-3 | 6.76E-6 | 4.52E-4 | 2.21E-5 |
| 256 | 65 | 3.69E+2 | 3.55E-4 | 1.22E-3 | 4.34E-7 | 8.50E-5 | 2.14E-6 |
| rate | | | $\mathcal{O}(h^{1.01})$ | $\mathcal{O}(h^{1.01})$ | $\mathcal{O}(h^{1.96})$ | $\mathcal{O}(h^{1.61})$ | $\mathcal{O}(h^{1.85})$ |

**6.3. Example 3.** In the third example we test a three dimensional problem with known analytic solution

$$p(x,y,z) = x + y + z - 1.5$$

and full tensor coefficient

$$K = \begin{pmatrix} x^2+y^2+1 & 0 & 0 \\ 0 & z^2+1 & \sin(xy) \\ 0 & \sin(xy) & x^2y^2+1 \end{pmatrix}.$$

Convergence rates are given in Tables 6.10 and 6.11, again confirming the theoretical results. Note that even though this is a problem with a full tensor $K$, the computed

Table 6.7

*Number of iterations, condition number, discrete norm errors and convergence rates for Example 2: discontinuous linear mortars and matching grids.*

| $1/h$ | *iter.* | *cond.* | $\|\|p-p_h\|\|$ | $\|\|\mathbf{u}-\mathbf{u}_h\|\|$ | $\|\|\|p-p_h\|\|\|$ | $\|\|\|\mathbf{u}-\mathbf{u}_h\|\|\|$ | $\|\|\|p-\lambda_H\|\|\|$ |
|---|---|---|---|---|---|---|---|
| 4 | 8 | 1.45E+1 | 2.35E-2 | 8.17E-2 | 1.51E-3 | 6.77E-2 | 4.58E-3 |
| 8 | 16 | 2.36E+1 | 1.15E-2 | 3.94E-2 | 4.15E-4 | 1.73E-2 | 1.16E-3 |
| 16 | 22 | 4.36E+1 | 5.69E-3 | 1.95E-2 | 1.06E-4 | 4.37E-3 | 2.92E-4 |
| 32 | 36 | 8.55E+1 | 2.84E-3 | 9.71E-3 | 2.69E-5 | 1.09E-3 | 7.32E-5 |
| 64 | 52 | 1.70E+2 | 1.42E-3 | 4.85E-3 | 6.75E-6 | 2.74E-4 | 1.82E-5 |
| 128 | 77 | 3.40E+2 | 7.10E-4 | 2.42E-3 | 1.72E-6 | 6.85E-5 | 4.71E-6 |
| 256 | 108 | 6.80E+2 | 3.55E-4 | 1.21E-3 | 4.20E-7 | 1.71E-5 | 1.14E-6 |
| rate | | | $\mathcal{O}(h^{1.01})$ | $\mathcal{O}(h^{1.01})$ | $\mathcal{O}(h^{1.97})$ | $\mathcal{O}(h^{1.99})$ | $\mathcal{O}(h^{1.99})$ |

Table 6.8

*Number of iterations, condition number, discrete norm errors and convergence rates for Example 2: continuous quadratic mortars and non-matching grids.*

| $1/h$ | *iter.* | *cond.* | $\|\|p-p_h\|\|$ | $\|\|\mathbf{u}-\mathbf{u}_h\|\|$ | $\|\|\|p-p_h\|\|\|$ | $\|\|\|\mathbf{u}-\mathbf{u}_h\|\|\|$ | $\|\|\|p-\lambda_H\|\|\|$ |
|---|---|---|---|---|---|---|---|
| 4 | 12 | 9.30E+1 | 1.84E-2 | 6.20E-2 | 1.13E-3 | 4.58E-2 | 3.27E-3 |
| 16 | 19 | 4.84E+1 | 4.37E-3 | 1.50E-2 | 8.06E-5 | 3.67E-3 | 2.41E-4 |
| 64 | 30 | 1.43E+2 | 1.08E-3 | 3.73E-3 | 5.38E-6 | 6.45E-4 | 2.45E-5 |
| 256 | 45 | 3.98E+2 | 2.72E-4 | 9.26E-4 | 3.70E-7 | 1.28E-4 | 2.97E-6 |
| rate | | | $\mathcal{O}(h^{1.01})$ | $\mathcal{O}(h^{1.01})$ | $\mathcal{O}(h^{1.93})$ | $\mathcal{O}(h^{1.40})$ | $\mathcal{O}(h^{1.68})$ |

Table 6.9

*Number of iterations, condition number, discrete norm errors and convergence rates for Example 2: continuous linear mortars and non-matching grids.*

| $1/h$ | *iter.* | *cond.* | $\|\|p-p_h\|\|$ | $\|\|\mathbf{u}-\mathbf{u}_h\|\|$ | $\|\|\|p-p_h\|\|\|$ | $\|\|\|\mathbf{u}-\mathbf{u}_h\|\|\|$ | $\|\|\|p-\lambda_H\|\|\|$ |
|---|---|---|---|---|---|---|---|
| 4 | 8 | 3.40E+1 | 1.84E-2 | 9.57E-2 | 5.23E-3 | 7.04E-2 | 5.23E-3 |
| 8 | 12 | 3.62E+1 | 8.83E-3 | 4.05E-2 | 3.29E-4 | 2.38E-2 | 1.45E-3 |
| 16 | 20 | 4.14E+1 | 4.37E-3 | 1.75E-2 | 8.20E-5 | 7.76E-3 | 3.53E-4 |
| 32 | 27 | 7.62E+1 | 2.18E-3 | 8.06E-3 | 2.03E-5 | 2.63E-3 | 8.77E-5 |
| 64 | 36 | 1.50E+2 | 1.09E-3 | 3.85E-3 | 5.17E-6 | 9.06E-4 | 2.17E-5 |
| 128 | 53 | 2.99E+2 | 5.44E-4 | 1.88E-3 | 1.31E-6 | 3.17E-4 | 5.45E-6 |
| 256 | 74 | 5.98E+2 | 2.72E-4 | 9.28E-4 | 3.18E-7 | 1.11E-4 | 1.36E-6 |
| rate | | | $\mathcal{O}(h^{1.01})$ | $\mathcal{O}(h^{1.11})$ | $\mathcal{O}(h^{2.12})$ | $\mathcal{O}(h^{1.55})$ | $\mathcal{O}(h^{1.99})$ |

rates exceed the predicted ones (e.g., for the discrete pressure error we expect rate of 1.25 but observe 2.02). The computed solution and error in pressure and velocity for the case of continuous quadratic mortars on the first level of refinement for matching grids are shown in Figure 6.3.

**6.4. Example 4.** In the fourth example we study the behavior of the method as we vary the number of subdomains and the degree of the mortar approximating functions. The analytic solution and the tensor coefficient are as in Example 1. The fine grid of $256 \times 256$ elements was split into three different domain decompositions (coarse grids) of $2 \times 2$, $4 \times 4$, and $8 \times 8$ subdomains. The mortar grids were chosen to be consistent with the optimal choice for velocity superconvergence, i.e., $H = h^{1/2}$ for quadratic mortars and $H = 2h$ for linear mortars.

TABLE 6.10

*Number of iterations, condition number, discrete norm errors and convergence rates for Example 3: continuous quadratic mortars and matching grids.*

| $1/h$ | *iter.* | *cond.* | $\|\|p - p_h\|\|$ | $\|\|\mathbf{u} - \mathbf{u}_h\|\|$ | $\|\|\|p - p_h\|\|\|$ | $\|\|\|\mathbf{u} - \mathbf{u}_h\|\|\|$ | $\|\|\|p - \lambda_H\|\|\|$ |
|---|---|---|---|---|---|---|---|
| 4 | 14 | 7.54E+0 | 4.33E-1 | 1.01E-1 | 1.87E-2 | 3.27E-3 | 1.42E-2 |
| 16 | 27 | 2.69E+1 | 1.08E-1 | 2.52E-2 | 1.09E-3 | 4.60E-4 | 8.38E-4 |
| 64 | 47 | 8.95E+1 | 2.71E-2 | 6.29E-3 | 6.69E-5 | 5.58E-5 | 5.17E-5 |
| rate | | | $\mathcal{O}(h^{1.00})$ | $\mathcal{O}(h^{1.00})$ | $\mathcal{O}(h^{2.03})$ | $\mathcal{O}(h^{1.47})$ | $\mathcal{O}(h^{2.02})$ |

TABLE 6.11

*Number of iterations, condition number, discrete norm errors and convergence rates for Example 3: discontinuous quadratic mortars and matching grids.*

| $1/h$ | *iter.* | *cond.* | $\|\|p - p_h\|\|$ | $\|\|\mathbf{u} - \mathbf{u}_h\|\|$ | $\|\|\|p - p_h\|\|\|$ | $\|\|\|\mathbf{u} - \mathbf{u}_h\|\|\|$ | $\|\|\|p - \lambda_H\|\|\|$ |
|---|---|---|---|---|---|---|---|
| 4 | 14 | 7.54E+0 | 4.33E-1 | 1.01E-1 | 1.87E-2 | 3.27E-3 | 1.42E-2 |
| 16 | 28 | 2.74E+1 | 1.08E-1 | 2.52E-2 | 1.09E-3 | 4.60E-4 | 8.38E-4 |
| 64 | 49 | 9.15E+1 | 2.71E-2 | 6.29E-3 | 6.69E-5 | 5.58E-5 | 5.17E-5 |
| rate | | | $\mathcal{O}(h^{1.00})$ | $\mathcal{O}(h^{1.00})$ | $\mathcal{O}(h^{2.03})$ | $\mathcal{O}(h^{1.47})$ | $\mathcal{O}(h^{2.02})$ |

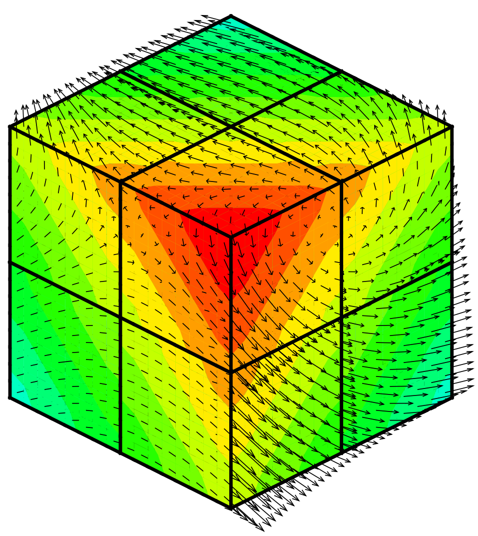

A. *Solution*

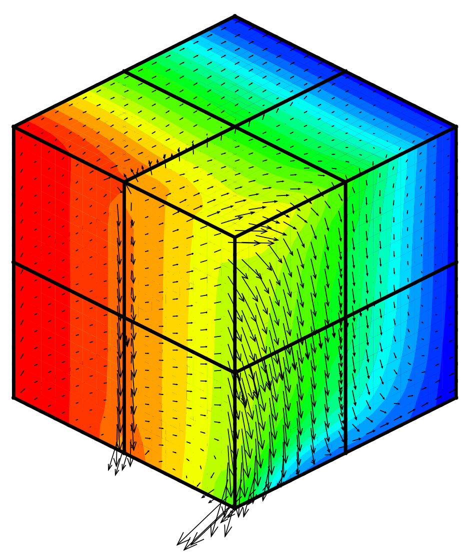

B. *Error*

FIG. 6.3. *Computed pressure (shade) and velocity (arrows) for Example 3: continuous quadratic mortars and matching grids.*

Convergence rates as well as approximate number of floating point operations (flops) for this test case are given in Tables 6.12 and 6.13. In reporting the flops, we neglected the relatively low cost of projecting to and from the mortar space and counted only the cost of the subdomain solves. Observe that when the number of subdomain elements increases, the degrees of freedom for the linear mortars increase faster than the degrees of freedom for quadratic mortars, so that the chosen way of counting the flops favors slightly the case of linear mortars.

We conclude from the results of this test case that while the errors are comparable for all domain decompositions, choosing a smaller coarse grid ($2\times 2$) is computationally more efficient than choosing a larger coarse grid ($8 \times 8$), since it reduces the amount of work by about 40%. In addition, for a given domain decomposition, a comparison between linear and quadratic mortars confirms again the better efficiency of the latter.

Similar results were observed for discontinuous (linear and quadratic) mortars.

TABLE 6.12
*Number of iterations, number of flops and discrete norm errors for Example 4: continuous linear mortars and multiple domains.*

| *dom.* | *iter.* | *flops* | $\|\|p - p_h\|\|$ | $\|\|\mathbf{u} - \mathbf{u}_h\|\|$ | $\|\|\|p - p_h\|\|\|$ | $\|\|\|\mathbf{u} - \mathbf{u}_h\|\|\|$ | $\|\|\|p - \lambda_H\|\|\|$ |
|---|---|---|---|---|---|---|---|
| 2x2 | 50 | 2.93E+8 | 4.97E-3 | 4.31E-3 | 1.62E-5 | 2.28E-5 | 1.36E-5 |
| 4x4 | 89 | 3.18E+8 | 4.97E-3 | 4.31E-3 | 1.65E-5 | 2.81E-5 | 2.28E-5 |
| 8x8 | 206 | 5.30E+8 | 4.97E-3 | 4.31E-3 | 1.98E-5 | 3.92E-5 | 4.53E-5 |

TABLE 6.13
*Number of iterations, number of flops and discrete norm errors for Example 4: continuous quadratic mortars and multiple domains.*

| *dom.* | *iter.* | *cond.* | $\|\|p - p_h\|\|$ | $\|\|\mathbf{u} - \mathbf{u}_h\|\|$ | $\|\|\|p - p_h\|\|\|$ | $\|\|\|\mathbf{u} - \mathbf{u}_h\|\|\|$ | $\|\|\|p - \lambda_H\|\|\|$ |
|---|---|---|---|---|---|---|---|
| 2x2 | 33 | 1.93E+8 | 4.97E-3 | 4.31E-3 | 1.62E-5 | 2.44E-5 | 1.39E-5 |
| 4x4 | 71 | 2.54E+8 | 4.97E-3 | 4.31E-3 | 1.67E-5 | 5.22E-5 | 2.50E-5 |
| 8x8 | 125 | 3.22E+8 | 4.97E-3 | 4.31E-3 | 1.74E-5 | 9.35E-5 | 4.33E-5 |

**6.5. Adaptive mesh refinement.** In the last two examples, we test the performance of the residual-based error estimator. The estimator is used as a local error indicator that drives an adaptive mesh refinement process. The following algorithm describes the adaptive procedure.

GRID REFINEMENT ALGORITHM

1. Solve the problem on a coarse subdomain and mortar grid.
2. For each subdomain $\Omega_i$:
   (a) Compute $\omega_i = \left( \sum_{E \in \mathcal{T}_{h,i}} \omega_E^2 + \sum_{\tau \in \mathcal{T}^{\Gamma_i,H}} \omega_\tau^2 \right)^{1/2}$;
   (b) If $\omega_i > .5 \max_{1 \le j \le n} \omega_j$, refine $\mathcal{T}_{h,i}$.
3. For each interface $\Gamma_{i,j}$, if either $\Omega_i$ or $\Omega_j$ has been refined $m$ times, refine $\mathcal{T}_{H,i,j}$.
4. Solve the problem on the refined grid. If either the desired error tolerance or the maximum refinement level has been reached, exit; otherwise, go to Step 2.

Note that we employ the pressure error estimator based on $\omega_E$ and $\omega_\tau$, defined in (5.7) and (5.8), since it provides an efficient and reliable estimate of the $L^2$ pressure error, due to Theorem 5.1 and Theorem 5.3 (see also Remark 5.2). Also, according to Step 3, the mortar grids are refined if either adjacent subdomain grid is refined sufficiently many times (depending on the mortar polynomial degree $m$).

For these last two examples, the unit square domain is decomposed into $6 \times 6$ subdomains. The coarse grid in each subdomain is $2 \times 2$ with a single mortar element on each interface. Both continuous and discontinuous piecewise quadratic mortar spaces on the interfaces were tested.

**6.5.1. Example 5.** In Example 5 we test a problem with a boundary layer. The true pressure is

$$p(x, y) = 1000\, x\, y\, e^{-10(x^2+y^2)},$$

with $K = I$. The computed pressures after three refinements for the cases of discontinuous linear and quadratic mortars are shown in Figure 6.4. Observe that the linear mortars produce finer grids that are appropriately refined along the boundary layer while the quadratic mortars give grids that are coarser and more uniform in that region.

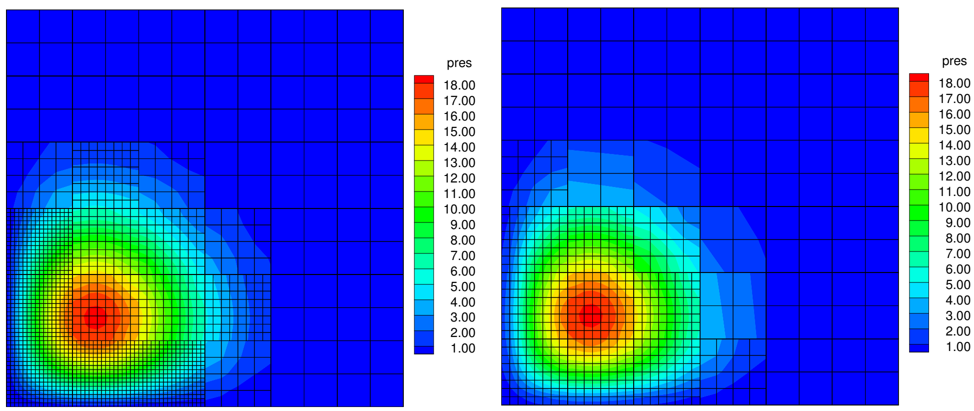


A. *Discontinuous linear mortars* B. *Discontinuous quadratic mortars*

FIG. 6.4. *Computed pressure on the fourth grid level for Example 5*

**6.5.2. Example 6.** In the last example we test a problem with a highly oscillating tensor

$$K = \begin{cases} 105 - 100\sin(20\pi x)\sin(20\pi y), & x, y \in [0, 1/2] \text{ or } x, y \in [1/2, 1], \\ 105 - 100\sin(2\pi x)\sin(2\pi y), & \text{otherwise.} \end{cases}$$

The computed magnitude of the velocity after four refinements for the cases of continuous linear and quadratic mortars are shown in Figure 6.5.

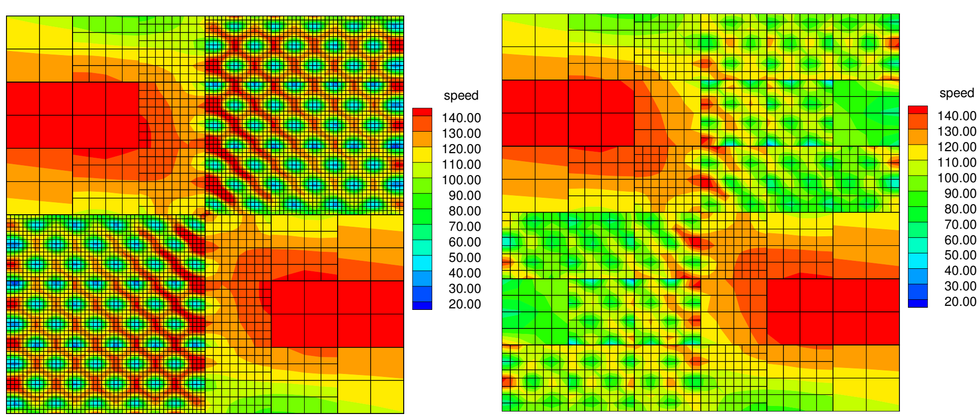


A. *Continuous linear mortars* B. *Continuous quadratic mortars*

FIG. 6.5. *Computed magnitude of the velocity on the fifth grid level for Example 6*

Note that the highly oscillating velocity is well resolved by the fine computational grid in the lower-left and the upper-right regions. Some refinement is also observed along the line $x = 1/2$ due to the large jump-flux term $\omega_\tau$. As in the previous example, linear mortars produce finer grids, especially in the two regions of high oscillation.

## REFERENCES


[1] J. E. Aarnes, *On the use of a mixed multiscale finite element method for greater flexibility and increased speed or improved accuracy in reservoir simulation*, Multiscale Model. and Simul., 2 (2004), pp. 421–439.

[2] J. E. Aarnes, S. Krogstad, and K.-A. Lie, *A hierarchical multiscale method for two-phase flow based upon mixed finite elements and nonuniform coarse grids*, Multiscale Model. Simul., (2006, to appear).

[3] T. Arbogast, *Analysis of a two-scale, locally conservative subgrid upscaling for elliptic problems*, SIAM J. Numer. Anal., 42 (2004), pp. 576–598.

[4] T. Arbogast and K. J. Boyd, *Subgrid upscaling and mixed multiscale finite elements*, SIAM J. Numer. Anal., (2006, to appear).

[5] T. Arbogast, L. C. Cowsar, M. F. Wheeler, and I. Yotov, *Mixed finite element methods on non-matching multiblock grids*, SIAM J. Numer. Anal., 37 (2000), pp. 1295–1315.

[6] T. Arbogast, C. N. Dawson, P. T. Keenan, M. F. Wheeler, and I. Yotov, *Enhanced cell-centered finite differences for elliptic equations on general geometry*, SIAM J. Sci. Comput., 19 (1998), pp. 404–425 (electronic).

[7] T. Arbogast, S. E. Minkoff, and P. T. Keenan, *An operator-based approach to upscaling the pressure equation*, in Computational Methods in Water Resources XII, Vol. 1: Computational Methods in Contamination and Remediation of Water Resources, V. N. Burganos et al., eds., Southampton, U.K., 1998, Computational Mechanics Publications, pp. 405–412.

[8] T. Arbogast, M. F. Wheeler, and I. Yotov, *Mixed finite elements for elliptic problems with tensor coefficients as cell-centered finite differences*, SIAM J. Numer. Anal., 34 (1997), pp. 828–852.

[9] T. Arbogast and I. Yotov, *A non-mortar mixed finite element method for elliptic problems on non-matching multiblock grids*, Comput. Meth. Appl. Mech. Eng., 149 (1997), pp. 255–265.

[10] D. N. Arnold and F. Brezzi, *Mixed and nonconforming finite element methods: Implementation, postprocessing and error estimates*, RAIRO Modél. Math. Anal. Numér., 19 (1985), pp. 7–32.

[11] C. Bernardi, Y. Maday, and A. T. Patera, *A new nonconforming approach to domain decomposition: The mortar element method*, in Nonlinear partial differential equations and their applications, H. Brezis and J. L. Lions, eds., Longman Scientific & Technical, UK, 1994.

[12] F. Brezzi, *Interacting with the subgrid world*, in Numerical Analysis, 1999, Chapman and Hall, 2000, pp. 69–82.

[13] F. Brezzi, J. Douglas, Jr., R. Duràn, and M. Fortin, *Mixed finite elements for second order elliptic problems in three variables*, Numer. Math., 51 (1987), pp. 237–250.

[14] F. Brezzi, J. Douglas, Jr., M. Fortin, and L. D. Marini, *Efficient rectangular mixed finite elements in two and three space variables*, RAIRO Modèl. Math. Anal. Numèr., 21 (1987), pp. 581–604.

[15] F. Brezzi, J. Douglas, Jr., and L. D. Marini, *Two families of mixed elements for second order elliptic problems*, Numer. Math., 88 (1985), pp. 217–235.

[16] F. Brezzi and M. Fortin, *Mixed and hybrid finite element methods*, Springer-Verlag, New York, 1991.

[17] Z. Chen and J. Douglas, Jr., *Prismatic mixed finite elements for second order elliptic problems*, Calcolo, 26 (1989), pp. 135–148.

[18] Z. Chen and T. Y. Hou, *A mixed multiscale finite element method for elliptic problems with oscillating coefficients*, Math. Comp., 72 (2003), pp. 541–576.

[19] P. G. Ciarlet, *The finite element method for elliptic problems*, North-Holland, Amsterdam, 1978. Studies in Mathematics and its Applications, Vol. 4.

[20] L. C. Cowsar, J. Mandel, and M. F. Wheeler, *Balancing domain decomposition for mixed finite elements*, Math. Comp., 64 (1995), pp. 989–1015.

[21] J. Douglas, Jr. and J. E. Roberts, *Global estimates for mixed methods for second order elliptic equations*, Math. Comp., 44 (1985), pp. 39–52.

[22] R. Durán, *Superconvergence for rectangular mixed finite elements*, Numer. Math., 58 (1990), pp. 287–298.

[23] R. E. Ewing, R. D. Lazarov, T. F. Russell, and P. S. Vassilevski, *Analysis of the mixed finite element method for rectangular Raviart-Thomas elements with local refinement*, in Third International Symposium on Domain Decomposition Methods for Partial Differential Equations, T. F. C. et al., ed., SIAM, Philadelphia, 1990, pp. 98–114.
[24] R. E. Ewing, R. D. Lazarov, and J. Wang, *Superconvergence of the velocity along the Gauss lines in mixed finite element methods*, SIAM J. Numer. Anal., 28 (1991), pp. 1015–1029.
[25] R. E. Ewing and J. Wang, *Analysis of mixed finite element methods on locally refined grids*, Numer. Math., 63 (1992), pp. 183–194.
[26] D. Gilbarg and N. S. Trudinger, *Elliptic partial differential equations of second order*, Springer-Verlag, Berlin, 1983.
[27] R. Glowinski and M. F. Wheeler, *Domain decomposition and mixed finite element methods for elliptic problems*, in First International Symposium on Domain Decomposition Methods for Partial Differential Equations, R. G. et al., ed., SIAM, Philadelphia, 1988, pp. 144–172.
[28] P. Grisvard, *Elliptic problems in nonsmooth domains*, Pitman, Boston, 1985.
[29] T. Y. Hou and X. H. Wu, *A multiscale finite element method for elliptic problems in composite materials and porous media*, J. Comput. Phys., 134 (1997), pp. 169–189.
[30] T. Y. Hou, X.-H. Wu, and Z. Cai, *Convergence of a multiscale finite element method for elliptic problems with rapidly oscillating coefficients*, Math. Comp., 68 (1999), pp. 913–943.
[31] T. J. R. Hughes, *Multiscale phenomena: Green's functions, the Dirichlet-to-Neumann formulation, subgrid scale models, bubbles and the origins of stabilized methods*, Comput. Methods Appl. Mech. Engrg., 127 (1995), pp. 387–401.
[32] T. J. R. Hughes, G. R. Feijóo, L. Mazzei, and J.-B. Quincy, *The variational multiscale method—a paradigm for computational mechanics*, Comput. Methods Appl. Mech. Engrg., 166 (1998), pp. 3–24.
[33] P. Jenny, S. H. Lee, and H. A. Tchelepi, *Multi-scale finite-volume method for elliptic problems in subsurface flow simulation*, J. Comp. Phys., 187 (2003), pp. 47–67.
[34] J. L. Lions and E. Magenes, *Non-homogeneous boundary value problems and applications*, vol. 1, Springer-Verlag, 1972.
[35] T. P. Mathew, *Domain decomposition and iterative refinement methods for mixed finite element discretizations of elliptic problems*, PhD thesis, Courant Institute of Mathematical Sciences, New York University, 1989. Tech. Rep. 463.
[36] M. Nakata, A. Weiser, and M. F. Wheeler, *Some superconvergence results for mixed finite element methods for elliptic problems on rectangular domains*, in The mathematics of finite elements and applications, V (Uxbridge, 1984), Academic Press, London, 1985, pp. 367–389.
[37] J. C. Nedelec, *Mixed finite elements in* $\mathbf{R}^3$, Numer. Math., 35 (1980), pp. 315–341.
[38] G. Pencheva and I. Yotov, *Balancing domain decomposition for mortar mixed finite element methods on non-matching grids*, Numer. Linear Algebra Appl., 10 (2003), pp. 159–180.
[39] R. A. Raviart and J. M. Thomas, *A mixed finite element method for 2nd order elliptic problems*, in Mathematical Aspects of the Finite Element Method, Lecture Notes in Mathematics, vol. 606, Springer-Verlag, New York, 1977, pp. 292–315.
[40] J. E. Roberts and J.-M. Thomas, *Mixed and hybrid methods*, in Handbook of Numerical Analysis, Vol. II, P. G. Ciarlet and J. Lions, eds., Elsevier Science Publishers B.V., 1991, pp. 523–639.
[41] L. R. Scott and S. Zhang, *Finite element interpolation of nonsmooth functions satisfying boundary conditions*, Math. Comp., 54 (1990), pp. 483–493.
[42] J. M. Thomas, Sur l'analyse numerique des methodes d'elements finis hybrides et mixtes, PhD thesis, Sciences Mathematiques, à l'Universite Pierre et Marie Curie, 1977.
[43] A. Weiser and M. F. Wheeler, *On convergence of block-centered finite differences for elliptic problems*, SIAM J. Numer. Anal., 25 (1988), pp. 351–375.
[44] M. F. Wheeler and I. Yotov, *A posteriori error estimates for the mortar mixed finite element method*, SIAM J. Numer. Anal., 43 (2005), pp. 1021–1042.
[45] B. I. Wohlmuth and R. H. W. Hoppe, *A comparison of a posteriori error estimators for mixed finite element discretizations by Raviart-Thomas elements*, Math. Comp., 68 (1999), pp. 1347–1378.
[46] I. Yotov, *Mixed finite element methods for flow in porous media*, PhD thesis, Rice University, Houston, Texas, 1996. TR96-09, Dept. Comp. Appl. Math., Rice University and TICAM report 96-23, University of Texas at Austin.